Journal of Medicinal Chemistry

Freie Universität Berlin

Subscriber access provided by UB + Fachbibliothek Chemie | (FU-Bibliothekssystem)

Article

Largazole Analogues Embodying Radical Changes in the Depsipeptide Ring: Development of a More Selective and Highly Potent Analogue

Jehad Almaliti, Ayad A Al-Hamashi, Ahmed T Negmeldin, Christin l Hanigan, Lalith Perera, Mary Kay H. Pflum, Robert A. Casero, and L. M. Viranga Tillekeratne

J. Med. Chem., **Just Accepted Manuscript** • DOI: 10.1021/acs.jmedchem.6b01271 • Publication Date (Web): 03 Nov 2016

Downloaded from http://pubs.acs.org on November 3, 2016

Just Accepted

"Just Accepted" manuscripts have been peer-reviewed and accepted for publication. They are posted online prior to technical editing, formatting for publication and author proofing. The American Chemical Society provides "Just Accepted" as a free service to the research community to expedite the dissemination of scientific material as soon as possible after acceptance. "Just Accepted" manuscripts appear in full in PDF format accompanied by an HTML abstract. "Just Accepted" manuscripts have been fully peer reviewed, but should not be considered the official version of record. They are accessible to all readers and citable by the Digital Object Identifier (DOI®). "Just Accepted" is an optional service offered to authors. Therefore, the "Just Accepted" Web site may not include all articles that will be published in the journal. After a manuscript is technically edited and formatted, it will be removed from the "Just Accepted" Web site and published as an ASAP article. Note that technical editing may introduce minor changes to the manuscript text and/or graphics which could affect content, and all legal disclaimers and ethical guidelines that apply to the journal pertain. ACS cannot be held responsible for errors or consequences arising from the use of information contained in these "Just Accepted" manuscripts.

ACS Publications

Journal of Medicinal Chemistry is published by the American Chemical Society. 1155 Sixteenth Street N.W., Washington, DC 20036

Published by American Chemical Society. Copyright © American Chemical Society. However, no copyright claim is made to original U.S. Government works, or works produced by employees of any Commonwealth realm Crown government in the course of their duties.

Largazole Analogues Embodying Radical Changes in the Depsipeptide Ring: Development of a More Selective and Highly Potent Analogue

Jehad Almaliti[ϕ§], Ayad A. Al-Hamashi[ϕ], Ahmed T. Negmeldin[±], Christin L. Hanigan[⊥], Lalith Perera[£], Mary Kay H Pflum[±], Robert A. Casero, Jr.[⊥], and L. M. Viranga Tillekeratne[ϕ]*

[ϕ]Department of Medicinal and Biological Chemistry, College of Pharmacy and Pharmaceutical Sciences, The University of Toledo, 2801, W. Bancroft Street, Toledo, OH-43606 USA

[§]Department of Pharmaceutical Sciences, Faculty of Pharmacy, The University of Jordan, Amman, 11942, Jordan.

[±] Department of Chemistry, Wayne State University, 5101 Cass Avenue, Detroit, Michigan 48202

[⊥] The Sidney Kimmel Comprehensive Cancer Center, The Johns Hopkins University School of Medicine, Bunting/Blaustein Cancer Research Building 1 1650 Orleans Street - Room 551, Baltimore, MD 21231

[£]Laboratory of Structural Biology, National Institute of Environmental Health Sciences, National Institutes of Health, Department of Health and Human Services, Research Triangle Park, North Carolina 27709

(A.T.N and C.L.H contributed equally to biological studies)

ABSTRACT

A number of analogues of the marine-derived histone deacetylase inhibitor largazole incorporating major structural changes in the depsipeptide ring were synthesized. Replacing the thiazole-thiazoline fragment of largazole with a bipyridine group gave analogue **7** with potent cell growth inhibitory activity and an activity profile similar to that of largazole, suggesting that conformational change accompanying switching hybridization from sp^3 to sp^2at C-7 is well tolerated. Analogue **7** was more class I selective compared to largazole, with at least 464-fold selectivity for class I HDAC proteins over class II HDAC6 compared to a 22-fold selectivity observed with largazole. To our knowledge **7** represents the first example of a potent and highly cytotoxic largazole analogue not containing a thiazoline ring. The elimination of a chiral center derived from the unnatural amino acid R-α-methylcysteine makes the molecule more amenable to chemical synthesis and, coupled with its increased class I selectivity, **7** could serve as a new lead compound for developing selective largazole analogues.

INTRODUCTION

Epigenetics is defined as heritable changes in gene expression that do not involve changes in the DNA sequence itself.[1] Epigenetic gene regulation includes DNA methylation and histone modifications, and non-coding RNA. This method of gene regulation is a vital part of normal development and cellular and tissue differentiation. Like many normal cellular processes, epigenetic regulation can become dysregulated in disease states. In cancer, aberrant silencing of tumor suppressor genes is a hallmark of tumorigenesis.[2] Since epigenetic regulation of genes does not change the DNA sequence, these aberrant changes can be targeted pharmacologically and reversed.

Histone modification as mentioned above is one mode of epigenetic regulation. Modification of histones' lysine residues include: methylation, acetylation and phosphorylation, which contribute to regulation of gene transcription.[3] Histone acetylation/deacetylation is one method of epigenetic regulation, which has been of interest to target pharmacologically. Acetylation and deacetylation of histones are controlled by two enzyme families; the histone acetyl transferases (HAT), which transfer acetyl groups from coenzyme A to lysine residues on histones and the histone deacetylases (HDAC), which catalyze the removal of acetyl groups from histone lysine residues. In general, acetylation of histones is associated with active transcriptionally competent euchromatin regions, while hypoacetylated histones mark transcriptionally inactive heterochromatic regions.[4] In cancer, aberrant gene silencing is associated with histone hypoacetylation and in some cases over-expression of HDAC proteins. Inhibition of HDAC proteins in some cancers could reactivate the silenced tumor suppresser genes and inhibit the growth of tumors.[5] Therefore, HDAC inhibitors have become a promising area of research in the development of selective drugs for the treatment of cancer. HDAC

inhibitors can block tumor cell proliferation by inducing cell differentiation, cell cycle arrest, and/or apoptosis.[6] Many nonhistone proteins are also substrates for HDAC thus underscoring their role in cellular process besides transcriptional regulation and their therapeutic potential in other non-cancer pathological conditions such as neurodegenerative diseases and immune/inflammatory disorders. [7–10] There are currently four HDAC inhibitors approved by the FDA for clinical use; suberoylanilide hydroxamic acid (SAHA) **1** (Figure 1) approved by the FDA in 2006 for the treatment of cutaneous manifestations of T-cell lymphoma,[11] FK228 **2** , approved in 2009 for the same disorder,[12] belinostat **3** approved in July 2014 for the treatment of peripheral T-cell lymphoma,[13] and very recently approved panobinostat **4** for the treatment of multiple myeloma.[14] There are at least 18 different isoforms of HDAC proteins belonging to four classes found in humans; the inhibitors FDA approved for cancer treatment to date all target either class 1 and/or class 2 HDAC enzymes.[15] SAHA, belinostat and panobinostat target class I and II HDACS, whereas FK228 is a class-I selective HDAC inhibitor. Selective HDAC inhibitors are warranted primarily to reduce side effects, target other disorders, and to probe the still not well understood physiological and pathological roles of different HDAC isoforms.[16] The structure-activity relationship (SAR) studies of HDAC inhibitors have revealed three essential domains required for a small molecule to act as an HDAC inhibitor; a zinc binding group which interacts with the zinc ion in the active site and precludes it from catalyzing the deacetylation process, a linker group, and a surface recognition cap group, which interacts with the hydrophobic residues on the rim of the active site.[17]

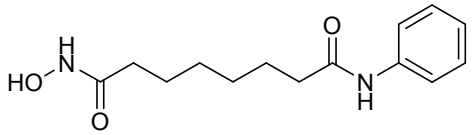

SAHA (1)

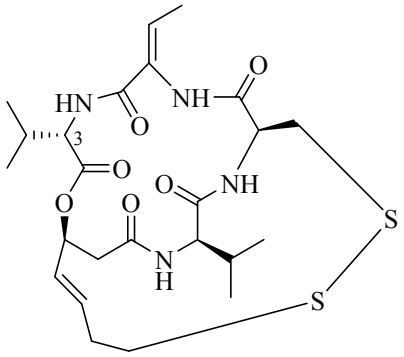

FK228 (2)

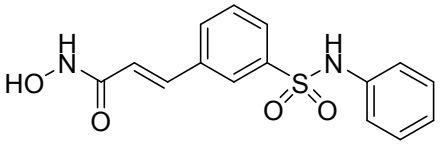

Belinostat (3)

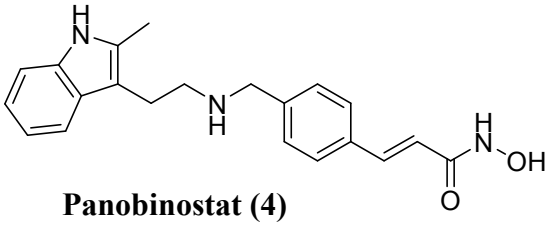

Panobinostat (4)

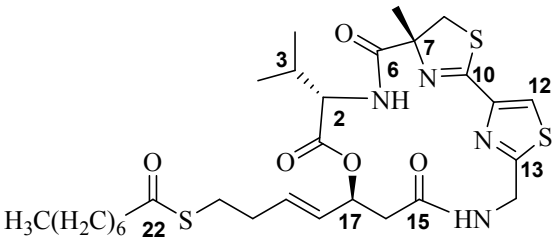

Largazole (5)

Figure 1. HDAC inhibitors and their pharmacophore.

Largazole **5** is a natural product isolated in 2008 from a marine cyanobacterium of the genus *Symploca* collected from Key Largo in Florida. Biological assays showed that largazole possesses potent growth inhibitory activity on several cancer cell lines and its effect on other disorders such as liver fibrosis, inflammation and rheumatoid arthritis is being evaluated[18–21]. Largazole is a class-I selective HDAC inhibitor and is a promising lead molecule in the

development of class/isoform selective HDAC inhibitors.[22] A number of largazole analogues has been synthesized and their biological activities evaluated delineating some of the structure-activity relationship (SAR) information of the molecule.[23–29] Modifications of the linker and the zinc binding group are not well tolerated and have mostly yielded less potent analogues.[27,30–32] In contrast, potent analogues have been generated by structural modification of the depsipeptide ring (surface recognition cap group).[28,30,31,33–35] The lower sequence homology between different HDAC isoforms at the surface near the opening to the binding pocket may be exploited to design more potent HDAC inhibitors by targeting the depsipeptide ring.[17]

Here in, we describe the synthesis and biological activity of novel largazole analogues with major modifications in the depsipeptide ring, while maintaining its 16-membered ring character (Figure 2). In analogue **6**, the thiazole-thiazoline moiety was replaced with a simple poly-ether linkage. Williams and coworkers reported that a pyridyl analogue in which the thiazole ring of largazole was replaced with a pyridine ring had enhanced HDAC inhibitory activity.[36] We synthesized analogue **7** in which a bi-pyridine moiety replaced the entire thiazole-thiazoline fragment of largazole. The bi-pyridine moiety introduces additional lipophilicity to the molecule, which may enhance interaction with the lipophilic rim of the active site. However, change in hybridization from sp^3 to sp^2 at C-7 position of largazole will impose significant conformational change in the depsipeptide ring of the molecule. In analogue **8**, the thiazole ring was replaced with a pyridine but the thiazoline moiety was replaced with a methylamine group. While the sp^2 nature of the thiazoline nitrogen is lost, the sp^3 configuration at C-7 was retained. Although there is a decrease in hydrophilicity, the N-methyl group provides a handle for structural manipulation to modulate hydrophilicity/lipophilicity in this part of the molecule. The analogue **9** which contains a benzyl-amine at this position was designed to determine the effect

of increasing bulk and lipophilicity at this position. As a further extension of this study, various electron donating and withdrawing groups can be introduced in the benzyl moiety in analogue **9**. With this in mind, analogues **10-13** with an electron withdrawing trifluoromethyl, an electron donating methoxy, an electron withdrawing and hydrophobic *p*-chloro, and a bulky 1-naphthyl group, respectively, were designed.

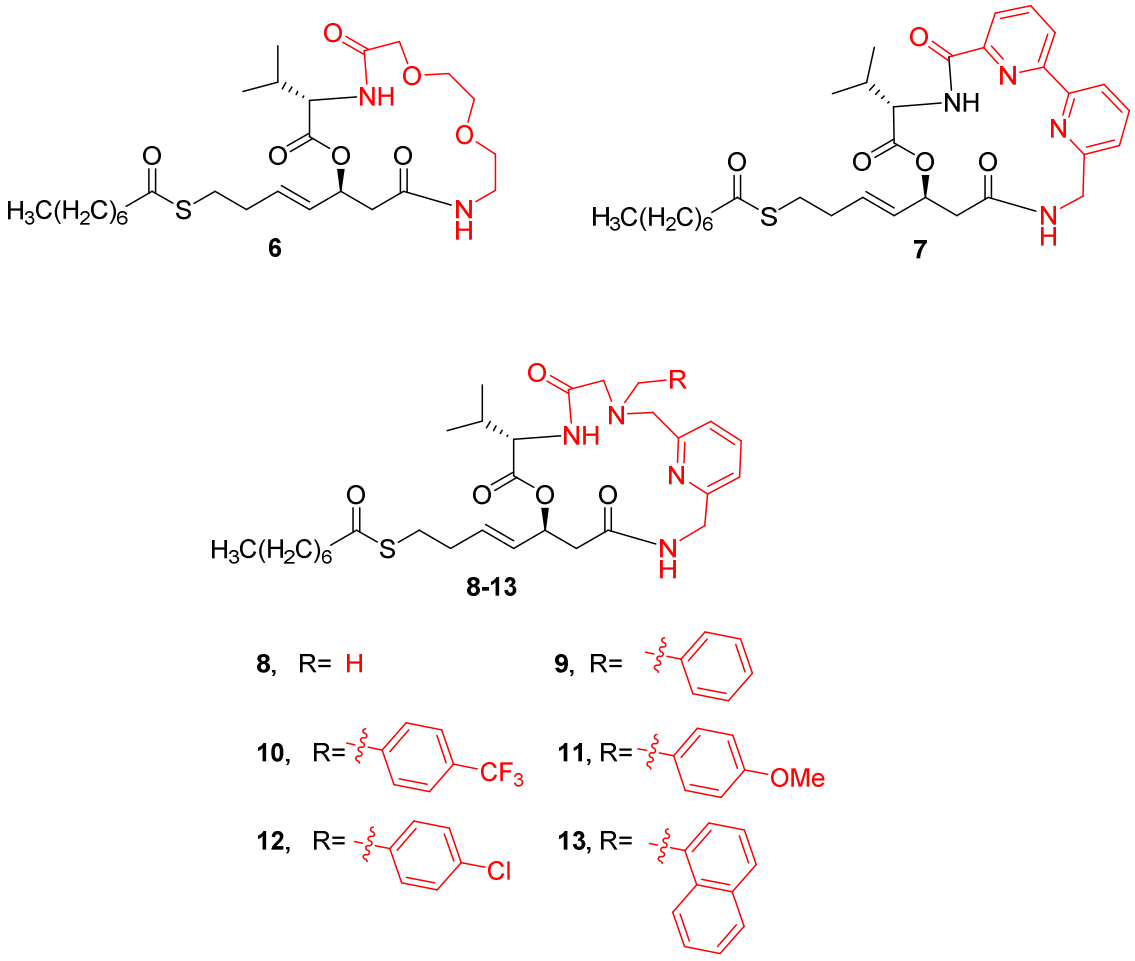

Figure 2. Largazole analogues synthesized

Chemistry:

From a synthetic view point, two major improvements were made in the convergent synthetic approach that we previously reported for largazole and analogues (Scheme 1).[27] First, an improved procedure for the synthesis of the thiol-containing linker moiety was developed to remove some of the limitations of our previous method.[27,28] Second, a new protection-deprotection protocol using mild conditions was developed to obtain the acyclic intermediate required for macrolactamization in pure form and in high yields. The closure of the 16-membered depsipeptide ring in largazole synthesis is challenging.[23] The macrocyclization yield is relatively low, and depends on the purity of the starting material and the reaction conditions.[37]. In the synthesis of analogues **12-13**, we used a new protection/deprotection strategy in which the carboxylic end was protected as a trimethylsilylethyl ester and the amino end was protected with Fmoc and both protecting groups were removed simultaneously under mild conditions using TBAF to obtain the deprotected intermediate in a high degree of purity and in high yields (vide infra). This simple protection-deprotection strategy may be employed successfully in other macrolactamization reactions as well.

Retrosynthetically, all analogues could be approached by acyl transfer from fragment **30** to amines **22-29**, followed by Yamaguchi esterification with Fmoc-valine to form acyclic precursors **14-21**. Macrolactamization and thio-esterification would give the target largazole analogues. The synthesis of the amine moieties **22-29** is described for each specific analogue.

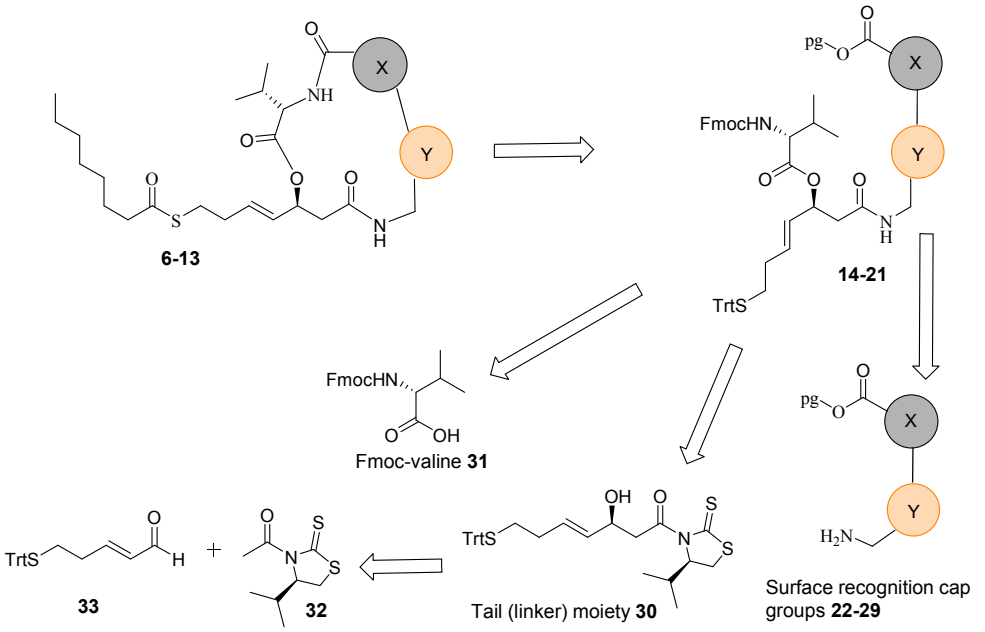

Analogue# (Intermediates #)	Analogue 6 (14/22/67/75)	Analogue 7 (15/23/68/76)	Analogue 8 (16/24/69/77)	Analogue 9 (17/25/70/78)	Analogue 10 (18/26/71/79)	Analogue 11 (19/27/75/80)	Analogue 12 (20/28/73/81)	Analogue 13 (21/29/74/82)
X					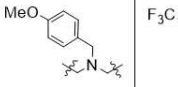	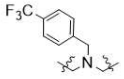	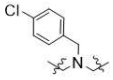	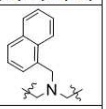
Y								
Pg	CH_3	CH_3	CH_3	CH_3	CH_3	CH_3	TMSE	TMSE

Scheme 1. Retrosynthetic analysis of largazole analogues **6-13.**

Michael addition of triphenylmethanethiol **34** to acrolein yielded aldehyde **36**, which was converted to the key aldehyde **33** in larger quantities and in higher yields using a Wittig reagent with a nitrile function as a masked aldehyde group (Scheme 2), instead of one containing an unmasked aldehyde group reported earlier.[27] Reaction of aldehyde **36** with (cyanomethyl)triphenylphosphonium chloride yielded an *E*:*Z*-mixture of nitrile **38**. Upon investigating varying experimental conditions, the highest ratio of the required *E*-isomer (5:1, *E*:*Z*) was obtained when the aldehyde **36** was reacted with (cyanomethyl)triphenylphosphonium chloride in benzene under reflux at 90 ^{o}C. Attempts to isomerize this mixture to the desired *E*

isomer in high yields under acidic and basic conditions were not successful. Therefore, the nitrile mixture was taken to the next step and reduced with DIBAL-H to an *E*/*Z* mixture (*E*:*Z*, 5:1) of the corresponding aldehydes.[38] Gratifyingly, the slow passage of the mixture through a silica column ensured complete isomerization to the desired *E*-isomer and the aldehyde **33** was obtained in 85% overall yield without the need for tedious separation procedures. Diastereoselective aldol reaction of the aldehyde **33** with acetyl Nagao auxiliary **32** gave alcohol **30**, the *S*-stereochemistry of the new chiral center of which was confirmed by Mosher ester analysis.[39]

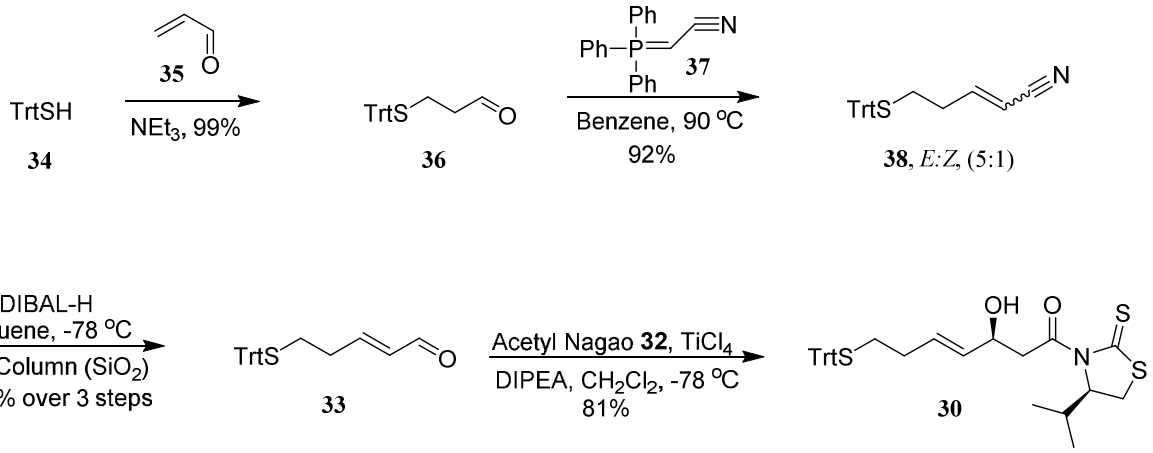

Scheme 2. Synthesis of intermediate **30**, the tail (linker) moiety.

The synthesis of the surface recognition cap moiety of analogue **6** is shown in scheme 3. As the alkylation of the N-Boc protected amino-alcohol **40** with methyl bromoacetate was sluggish, Finkelstein conditions were used to prepare the polyether **43** in 78% yields.[40] Removal of the Boc protecting group gave the amine **22** as its TFA salt, which was used in the next step without further purification.

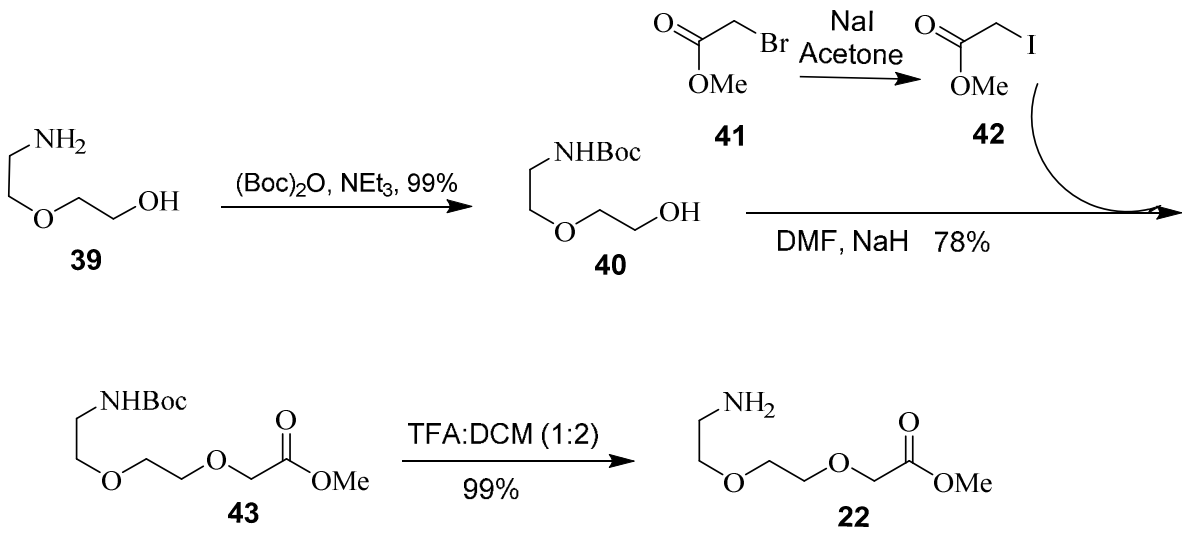

Scheme 3. Synthesis of amine **22** required for depsipeptide ring of analogue **5**.

For the synthesis of the surface recognition moiety of analogue **7**, 2-bromo-6-methylpyridine **44** was converted to the tin derivative **45** by reaction with n-Bu-Li followed by trimethyltin chloride (Scheme 4). Stille coupling of the tin derivative **45** with 2,6-dibromopyridine **46** in the presence of $Pd(PPh_3)_4$ catalyst gave 6-bromo-6'-methyl-2,2'-bipyridine **47**. A modified Jones oxidation procedure using chromium oxide in concentrated sulfuric acid was used to obtain the carboxylic acid **48** in high yields after working up the reaction mixture with cold ice water to precipitate out the pure carboxylic acid.[41] Esterification, followed by reaction with potassium cyanide in the presence of CuCN under microwave heating gave the corresponding nitrile **50** in high yields.[41] Nitrile **50** was reduced to methyl amine **23** by catalytic hydrogenation.

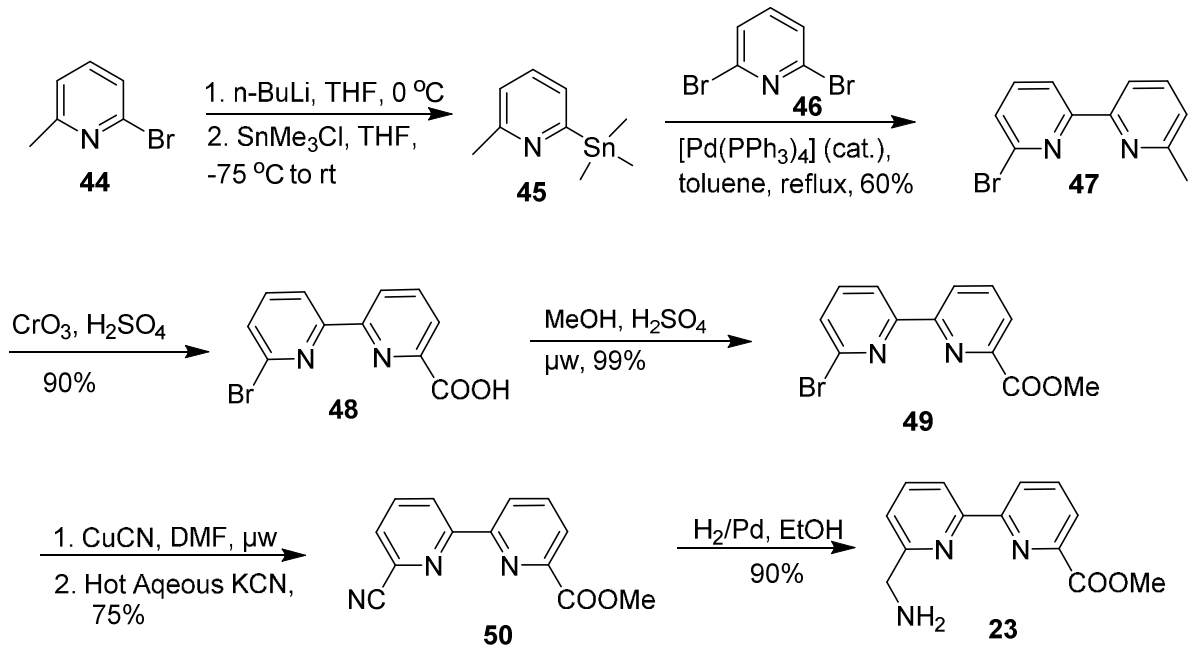

Scheme 4. Synthesis of amine **23** required for depsipeptide ring of analogue **7**.

To synthesize the surface recognition cap moiety for analogue **8-13**, 2,6-dihydroxymethyl pyridine **51** was treated with silver oxide and potassium iodide followed by tosyl chloride at -20 °C (Scheme 5) to obtain predominantly the mono-tosylated product **52**, with a trace amount of di-tosylated by-product.[42] After purification by passing through a pad of silica gel, compound **52** was converted to azide **53** by heating with sodium azide in DMF. Compound **53** was reacted with tosyl chloride and sodium hydroxide to give intermediate **54**, which was used to alkylate the secondary amines **55-60** yielding the tertiary amines **61-66**. They were reduced with H_2/Pd to give amines **24-29** in almost quantitative yield.

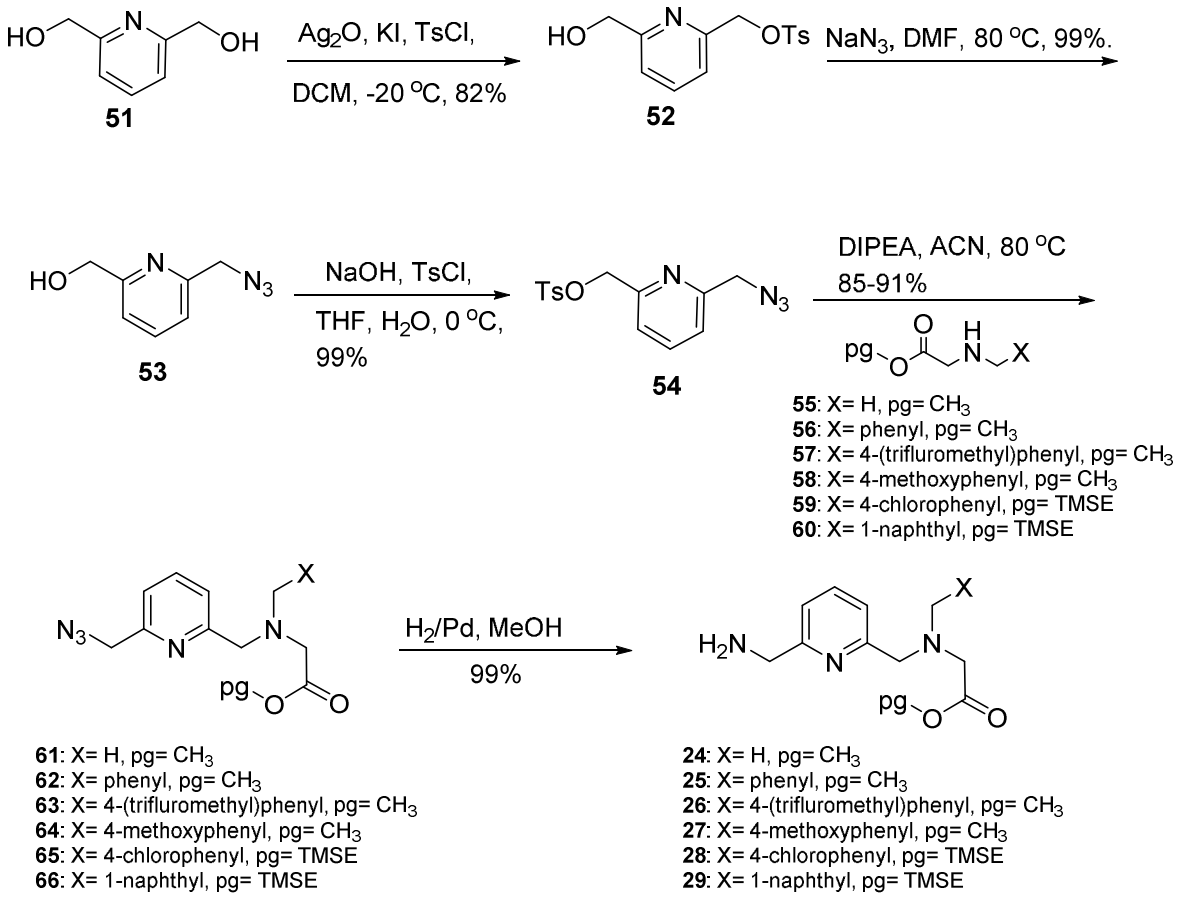

Scheme 5. Synthesis of amines **24-29** required for depsipeptide ring of analogues **8-13**.

With the required building blocks in hand, we proceeded to synthesize each analogue **6-13** by the general approach as shown in Scheme 6. Acyl transfer from **30** to amines **22-29** was carried out in the presence of DMAP to obtain alcohols **67-74**. They were esterified with Fmoc-L-valine using Yamaguchi esterification conditions to afford esters **14-21**. Esters **14-19** were saponified with aqueous LiOH and Fmoc group was removed with diethylamine, while in esters, **20-21** both trimethylsilylethyl ester and Fmoc groups were simultaneously removed with TBAF. The deprotected acyclic intermediates were macrolactamized using HOAt, HATU, and Hunig's base to afford the macrocyclic depsipeptide intermediates **75-82**.[37] The trityl group was removed

with TFA and the resulting thiols were dried azeotropically with toluene and esterified with octanoyl chloride. The products were purified by reversed phase chromatography on C_{18} in acetonitrile/water to obtain analogues **6-13**.

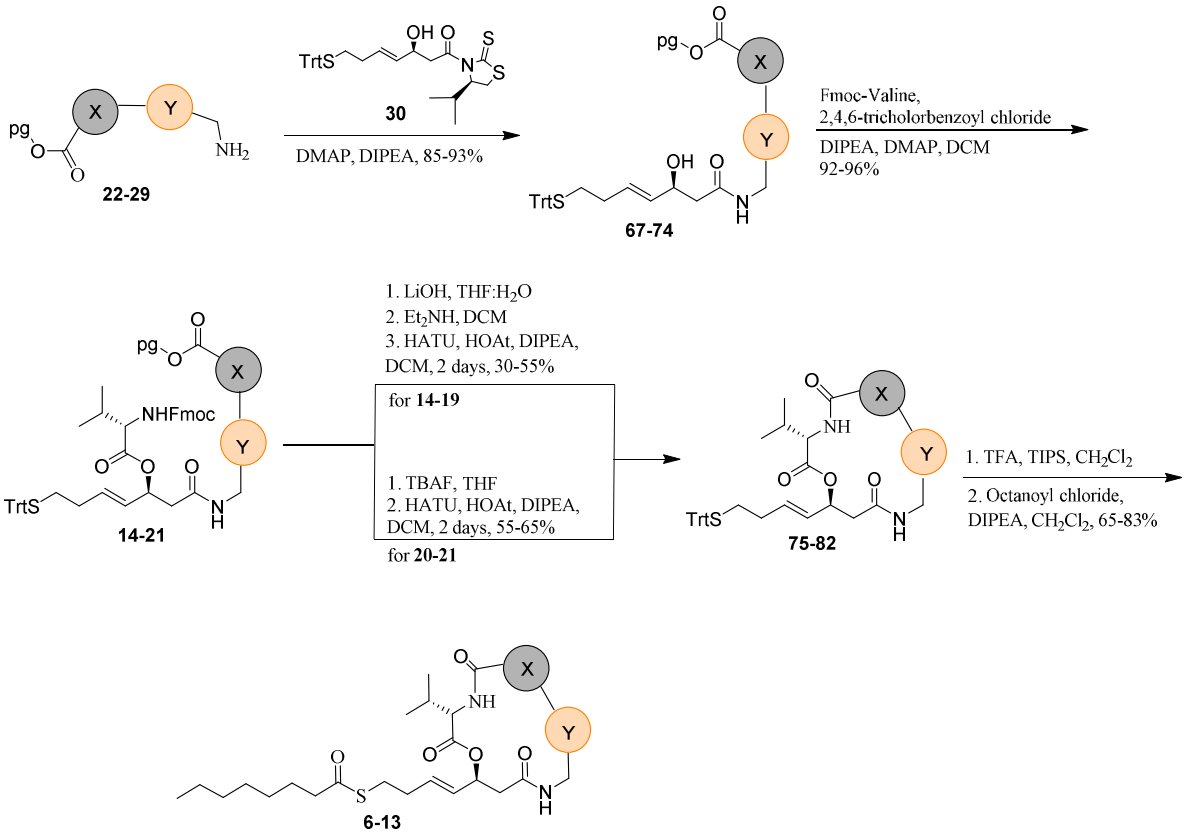

Analogue# (Intermediates #)	Analogue 6 (14/22/67/75)	Analogue 7 (15/23/68/76)	Analogue 8 (16/24/69/77)	Analogue 9 (17/25/70/78)	Analogue 10 (18/26/71/79)	Analogue 11 (19/27/75/80)	Analogue 12 (20/28/73/81)	Analogue 13 (21/29/74/82)
X					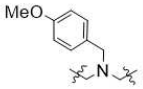	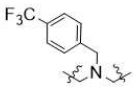	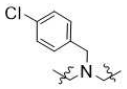	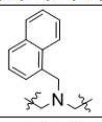
Y					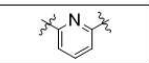	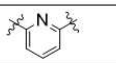	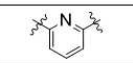	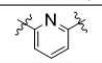
Pg	CH_3	CH_3	CH_3	CH_3	CH_3	CH_3	TMSE	TMSE

Scheme 6. Synthesis of largazole analogues **6-13**.

BIOLOGICAL STUDIES

Analogues **6-13** were subjected to preliminary screening of antiproliferative activity in a colon adenocarcinoma cell line (HCT116) by a standard 3-(4,5-dimethylthiazol-2-yl)-5-(3-carboxymethoxyphenyl)-2-(4-sulfophenyl)-2*H*-tetrazolium (MTS) reduction assay (Promega) using largazole as the control, as reported earlier.[27,43] The cells were incubated for 96 h with the analogues at 0.1 nM, 1 nM, 10 nM, 100 nM, 1 μM, and 5 μM concentrations. The results of the MTS assay for largazole and analogues **6** – **8** are shown in Figure 3. Largazole inhibited the growth of HCT116 cells with a GI_{50} of 65 nM, while the bi-pyridine analogue **7** with a GI_{50} of 75 nM showed an activity profile similar to that of largazole, and was the most active of the three analogues (see Figure **5a** below for a comprehensive list of GI_{50} values on NCI 60 cell lines). The poly-ether analogue **6** with major changes in the surface recognition cap group was less active than analogue **7** and largazole and but had moderate antiproliferative activity with a GI_{50} of 0.75 μM. on HCT 116 cells. Analogue **8** too showed moderate antiproliferative activity, with a GI_{50} value of 0.8 μM on HCT 116 cells.

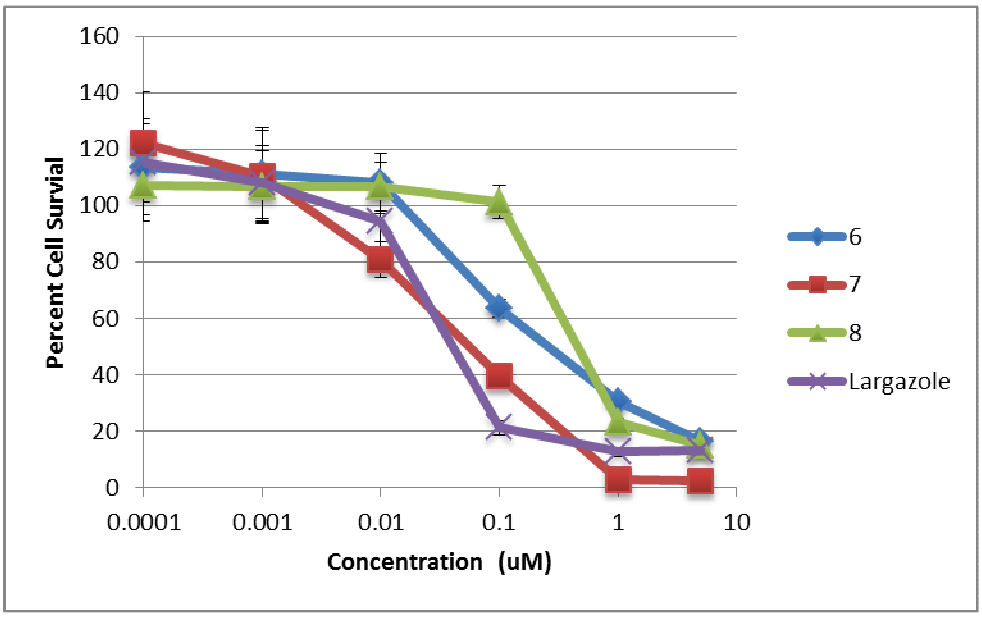

Figure 3. Cell survival MTS assay on HCT116 colorectal cancer cell line, treated for 96 hours at 0.1 nM, 1 nM, 10 nM, 100 nM, 1 μM and 5 μM. Each point represents the mean of three experiments; each with 4 replicates with the error bars indicating the SEM

Replacing the thiazoline ring of largazole with a methylamine group in analogue **8**, in addition to change of hybridization of the nitrogen atom, involved loss of hydrophobicity in this region of the molecule. Therefore, the benzylamine analogue **9** was designed to determine the effect of increasing bulk and lipophilicity at this position. As a further extension of this study, analogues **10** – **13** with electron withdrawing trifluoromethyl, electron donating methoxy, a hydrophobic *p*-chloro, and hydrophobic and bulky 1-naphthyl group, respectively, were designed to investigate the effect of altering electronic and steric properties at this position. However, all these structural modifications resulted in analogues with reduced levels of activity (Table 1 and in supporting informaiton, see figure S1 for growth inhibitory effect of analogues **9-13** on HCT 116 cells).

Table 1. GI_{50} values of MTS assay on survival of HCT116 colorectal cancer cell line treated with largazole and analogues **6-13** for 96 hours at 0.1 nM, 1 nM, 10 nM, 100 nM, 1 μM and 5 μM (See Figure 3 and Figure S1 in supporting information).

Compound	GI_{50} values (μM)
Largazole	0.065 ± 0.003
6	0.75 ± 0.017
7	0.075 ± 0.0002
8	0.8 ± 0.048
9	>5
10	3.2 ± 0.125
11	4.25 ± 0.063
12	2.67 ± 0.065
13	>5

All the analogues were tested in the National Cancer Institute (NCI) sixty human tumor cell line assay (NCI-60), where the antiproliferative activities of the compounds were screened initially at a single dose of 10 μM (Figure 4 and Figures S2 – S9 in supporting information).[44] Analogue **7** was the most active of the three compounds **6**-**8**. The mean percentage growth for analogues **6** and **8** were 38.58 and 40.77, respectively, which amounted to a 60% inhibition of the growth of all the cancer cell lines on average at 10 μM. In contrast, the mean percentage growth for analogue **7** was -16.18, suggesting strong antiproliferative and cytotoxic activity. However, analogues **6** and **8** exhibited moderate inhibitory activity on some of the melanoma, renal and leukemia cancer cell lines, but were less active on other cancer cell lines. Analogues **9** – **13** had mean percentage growths of -4.39, 0.43, 5.41, 1.42 and 34.86, respectively (Figures S5-S9 in supporting information). In the dose response assay against the 60 NCI cell lines, analogues **6** and **8** and **9-13** had moderate activity (micromolar GI_{50}s) on most of the cancer cell lines (Figure S10a in supporting information), and did not proceed to in vivo testing at the NCI. However, the benzyl and substituted benzyl analogues **9-12** were found to be several folds more active than the methylamine analogue **8** on most of the cell lines and the electron donating or withdrawing nature of the substituents did not seem to have an effect on activity. However, the presence of a bulky and hydrophobic chlorine atom in the para position in analogue **12** caused a significant reduction in activity, which was further compromised by the replacement of the phenyl group with an even bulkier and more hydrophobic naphthyl group leading to almost complete loss of activity.

In contrast, analogue **7** inhibited the growth of most of the cancer cell lines at concentrations <10 nM, (Figure 4 and Figure S10). The cytotoxicity profile of **7** is similar to that

of largazole and it was differentially more toxic to some of the ovarian, colon, and melanoma cancer cell lines at concentrations < 10 nM.[45]

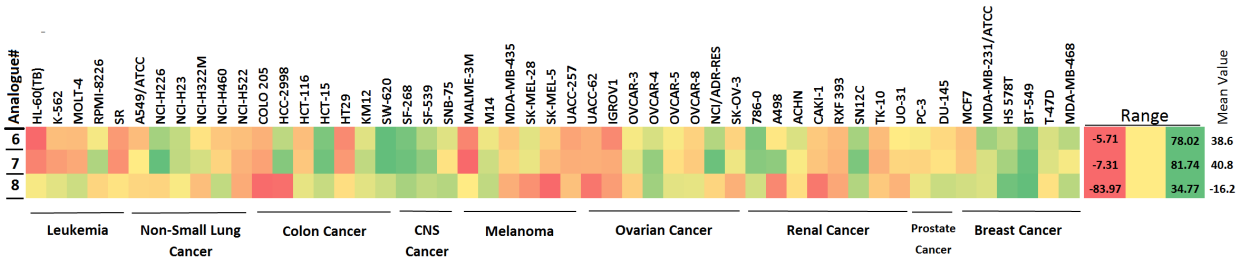

Figure 4. Heat map showing the antiproliferative activity of **6**-**8** in the NCI 60 cell line assay at 10 μM

As the antiproliferative activity of the synthesized analogues is most likely to be mediated through HDAC inhibition as in largazole, global histone H3 lysine 9 (H3K9) acetylation was evaluated by Western blot analysis of colorectal cancer cell line HCT116 after 24 h of cellular exposure at 10 nM, 100 nM, and 1 μM concentrations for each compound (Figure 5) as reported earlier.[27] Significant induction of global acetylation was observed by exposure to analogue **7** and largazole at 10 nM, and analogues **6** and **8** at 100 nM. These results are consistent with the results of the antiproliferative assay that **7** is more active than **6** and **8**.

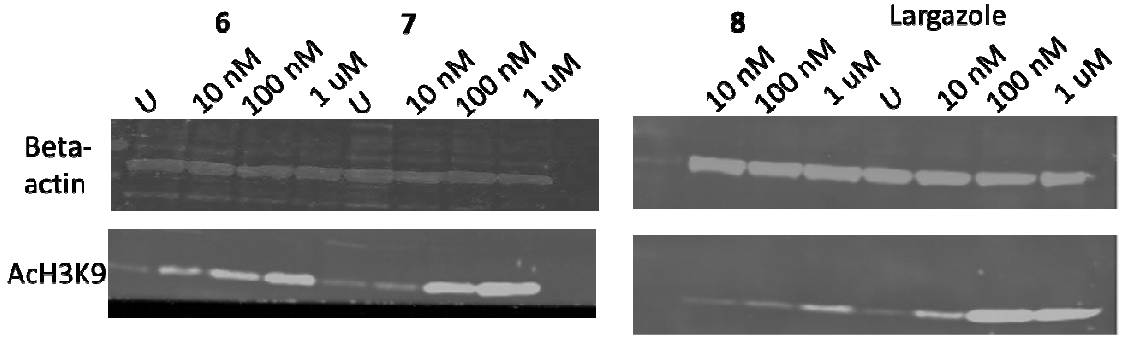

Figure 5. All compounds induced global changes of histone acetylation at varying concentrations. **7** showed the most comparable induction of global acetylation to largazole.

Western blot analysis of global histone H3 acetylation following the treatment of HCT116 cells with largazole and its analogues **6**-**8** (concentrations are 10, 100 nM and 1 μM). The Western blot is a representative figure from an experiment done 3 times.

Consistent with the results of the antiproliferative assay, analogues **9** – **12** induced less global histone acetylation than analogue **7** and largazole at 10 nM, and hardly any global acetylation was observed with the naphthyl analogue **13** even at 100 nM (Figure S13 in supporting information).

The HDAC inhibitory activity of the synthesized analogues was determined using an ELISA-based HDAC activity assay and mammalian cell derived HDAC1, HDAC2, HDAC3 and HDAC6 (Figure 6).[46] These assays were conducted after incubation of the test compound with each isoform for 15 minutes before the addition of the HDAC-Glo™ substrate. In a single concentration screen, analogues **6** (at 2 μM) and **7** (at 250 nM) inhibited Class I recombinant enzymes HDAC1, HDAC2 and HDAC3 significantly, while the Class II enzyme HDAC6 was relatively unaffected. The selectivity profile was similar to that of largazole tested at 1 μM. However, analogue **8** (1 μM) showed slightly greater inhibition of HDAC6 compared to **6** and **7**, suggesting that analogue **8** is less class I selective. Consistent with the antiproliferative activity results, analogues **9** – **13** showed lower inhibitory activity and lower selectivity on the enzymes, compared to **6**-**8**.

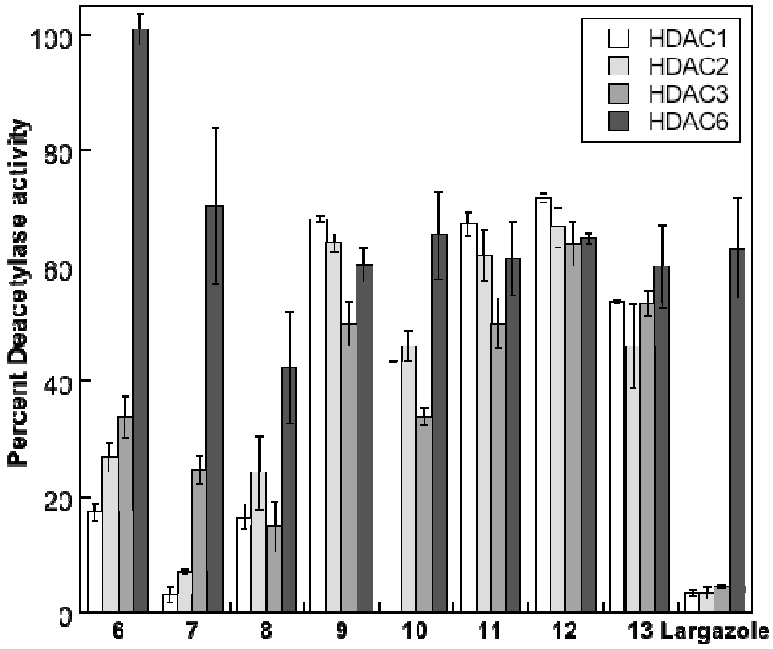

Figure 6. Isoform selectivity screen of analogues **6-13** and largazole against HDAC1, HDAC2, HDAC3, and HDAC6 at a single concentration of 2 μM for **6** and **13**, 250 nM for **7**, **9**, **11** and **12**, 1 μM for **8**, **10** and largazole. Mean percent of deacetylase activity remaining from at least two independent trials with standard errors were plotted (Table S14 in supporting information).

To further assess selectivity, IC_{50} values were determined for both largazole and the most potent analog **7** (Table 2). Largazole showed at least 22-fold selectivity for class I HDAC proteins over Class II HDAC6. Both the IC_{50} values and the fold selectivity of largazole are consistent with prior literature reports.[36,37] Interestingly, analogue **7** showed higher potency and selectivity for class I HDACs than largazole, with at least 464-fold selectivity for HDAC1, HDAC2, and HDAC3 over HDAC6 (Table 2).

Table 2. IC_{50} values of largazole and **7** with HDAC1, HDAC2, HDAC3, and HDAC6.[a]

Compound	IC_{50} values (nM)			
	HDAC1	HDAC2	HDAC3	HDAC6
Largazole	61 ± 7	64 ± 5	50 ± 6	1400 ± 100
7	21 ± 1	28 ± 1	27 ± 2	13000 ± 2000

[a] Mean IC_{50} value and standard error of at least two independent trials are shown (Figures S15 and S17 and Tables S16 and S18 in supporting information).

Analogue **7** was selected for in vivo studies in the Developmental Therapeutics Program of the NCI. In the nontumored animal toxicity assay for acute toxicity, no signs of toxicity was observed with **7** at the highest dose of 50 mg/kg tested.[44] Further in vivo testing is in progress at the NCI.

Molecular Modeling

In our previous study[28] we obtained a reasonable solution structure for largazole bound to HDAC-8 using a 30 ns MD trajectory with explicit water molecules . That study was based on the X-ray crystal structure (pdb ID:3RQD),[6] in which two largazole thiol molecules were bound to two HDAC-8 molecules. In the binding conformation, not only the two largazole thiol molecules were in contact with each other, but also both HDAC-8 peptides were in contact with each largazole thiol molecule, possibly making this binding pose somewhat adulterated. During molecular dynamics, we observed that the position of the macrocyclic ring of one largazole thiol molecule was shifted towards the area primarily occupied by the second largazole thiol molecule. In the present study, we used available X-ray crystal coordinates for HDAC-1 {pdb ID: 4BKX}[47]

and HDAC-2 {pdb ID: 4LY1}[48] as starting structures to study largazole and analogue **7** binding on these HDAC proteins tested in the study. However, only a partial X-ray crystal structure for HDAC-6 is currently available in the pdb database and therefore, within the context of the present computational study we did not pursue on looking at the binding of largazole and the analogue **7** in the ligand binding site of HDAC-6. As has been the case for their amino acid sequences (in supporting information Figure S19), overall structural features of HDAC-1 and HDAC-2 compared with HDAC-8 are quite similar to each other as displayed in Figure 7. After introducing largazole thiol onto HDAC-1 and HDAC-2 ligand binding sites using the largazole thiol bound HDAC-8 solution structure, each resultant system was subjected to a lengthy solution MD simulation to evaluate its binding behavior. In addition, a parallel set of simulations was performed after appropriately modifying the structure of largazole thiol in each of the above systems to yield the thiol of analogue **7** to elucidate its binding behavior in HDAC-1 and HDAC-2.

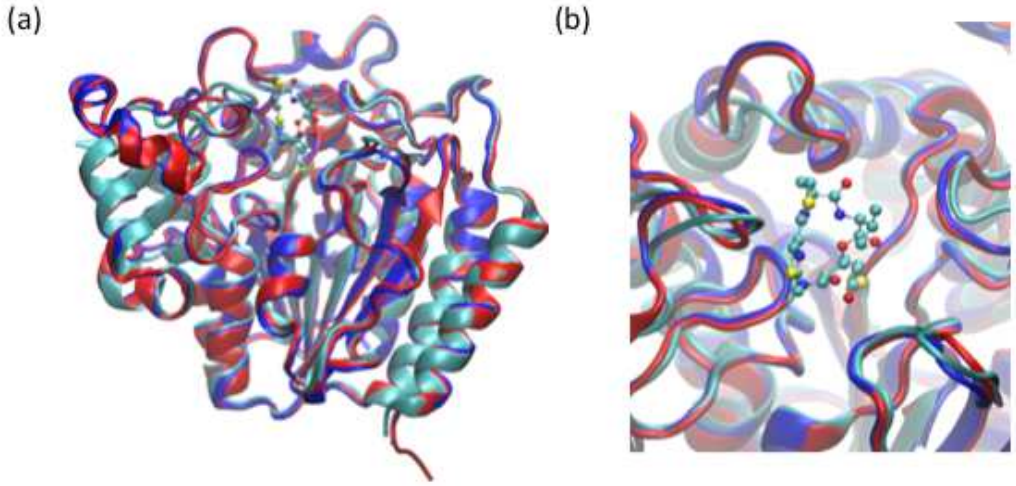

Figure 7. (a) Structural alignments of the X-ray crystal structures of HDAC-1 (pdb ID: 4BKX; in red) and HDAC-2 (pdb ID: 4lY1; in blue) with HDAC-8 (pdb ID: 3RQD; in cyan). The largazole thiol molecule from largazole thiol-bound HDAC-8 solution structure is also shown (in ball and stick representation) (b) The area of the binding site is zoomed in for a closer examination. All segments that can be in contact with the ligand are remarkably similar in structures. The loop directly above largazole thiol is seen to be different from that of the HDAC-1 and HDAC-2 and became involved in ligand interactions during the MD simulation of largazole thiol/HDAC-8.

To evaluate the properties of isolated ligands used in the molecular modeling, we first geometry optimized the thiols of largazole and analogue **7** (**7**-thiol) and calculated the point charge distribution using the CM5 charge derivation scheme introduced by Truhlar and coworkers[49] which works relatively accurately for systems with buried atoms. Two orthogonal views of optimized structures of largazole thiol and **7**-thiol are shown in Figure 8 with the color code using partial atomic charges. As can be seen from this figure, the part of the analogue molecule embedded into HDACs shows remarkable similarities in both structure and charge to that of largazole thiol. Stability of the protein-ligand complexes during molecular dynamics simulations is confirmed from the root mean square deviations (RMSD) calculated using the last 40 ns segments of each MD trajectory (see Figure 9).

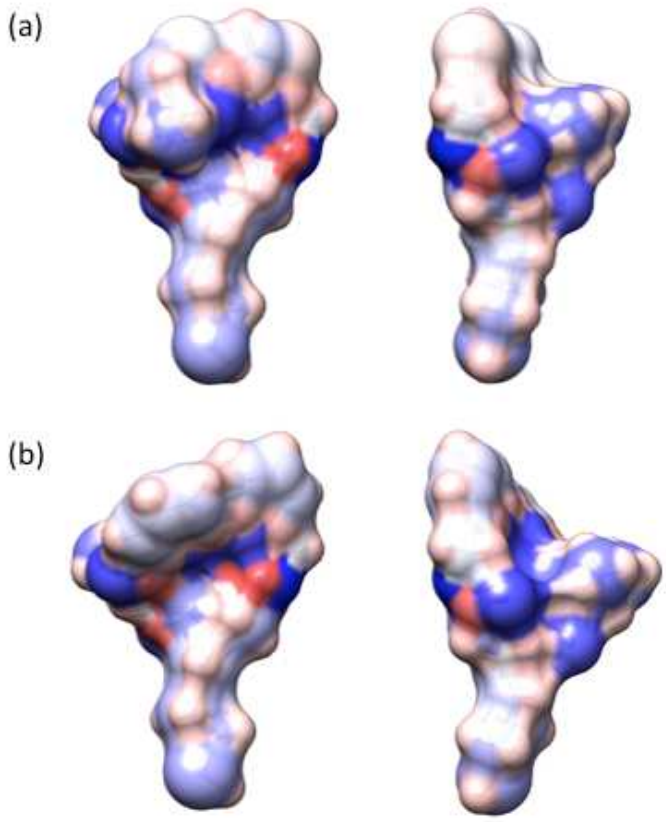

Figure 8. Optimized structures of (a) largazole thiol and (b) **7**-thiol. The values of the point charges at the atomic positions are used in the color coding. Two orthogonal orientations are given for each compound.

From the plot of RMSD values calculated using backbone heavy atoms after aligning them with the X-ray crystal structure versus the time (Figure 9), one can observe the type of fluctuations expected from a stable solution structure of a receptor protein in its ligand bound conformations. Average fluctuations are reasonable (< 2 Å) for peptides of this size during the solution dynamics and the analogue bound conformation shows slightly more stability compared to the largazole thiol-bound HDACs. Since RMSD provides information on the global stability

of the solvated complex, we have further evaluated the position fluctuations of each residue that were estimated as the B-factors from the last 30 ns of the MD trajectory for each HDAC system. The B-factors, representing average positional fluctuations plotted here against the residue ID (in supporting information, Figure S20), are the values calculated for all the back bone heavy atoms in each residue. Not many specific variations in B-factors among ligand/HDAC complexes are observed. When there are variations, they need to be looked at with respect to residues that are in contact with each ligand (largazole thiol or the analogue). From the previous MD simulation of the largazole thiol/HDAC-8 complex, we found K33, Y100, D101, H143, G151, F152, H180, F208, D267, M274, G302, and Y306 residues of HDAC-8 are in contact with largazole thiol. We emphasize here that K33 is not in contact with HDAC-8 in the X-ray crystal structure, but during dynamics it came in contact with largazole thiol. All the corresponding residues of the two HDACs can be found in the contact residue list of largazole thiol and **7**-thiol bound to HDAC-1 and HDAC-2 (see Table 3). Note here that residues P29 and H28 (in most cases) in HDAC-1 and HDAC-2 are in the loop corresponding to the one that contains K33 of HDAC-8.

In Figure 10, we display typical binding configurations for largazole thiol and **7**-thiol in HDAC-1 and HDAC-2. Except for the residues H28 and P29 in the N-terminal region, other residues listed in Table 3 participate in the common stem region and the macrocycle segment of largazole thiol and **7**-thiol. Largazole thiol in both HDACs seems to be more upright at the top part of the macrocycle and corresponding macrocyclic ring segment of **7**-thiol adopts a slightly tilted conformation (note that the planes of the two rings are also at an angle to each other). Also, we note that the atomic fluctuations of heavy atoms of largazole thiol are quite similar to one another in the two HDAC proteins. Though the values are slightly larger, especially for the atoms in the macrocyclic ring, than for largazole thiol, **7**-thiol (See supporting information,

Figure S21) also has quite similar atomic fluctuations in the two HDACs. This information points to rather similar binding interactions for each compound in the two slightly different protein environments. However, most significant information results from the enthalpy calculations carried out for the four simulations described in the methods. From the results summarized in the Table 4, largazole thiol is about 3-4 kcal/mol more stable in the protein environment as opposed to it being solvated in water. The difference in interaction strength is only slightly over one kcal/mol for this ligand. For **7**-thiol, this difference becomes only half a kcal/mol for the two proteins, but in the protein environment the analogue is more stable by about 6 kcal/mol. Also note that with this force field, for **7**-thiol, one can estimate approximately 2 kcal/mol more favorable interaction energy between water molecules when compared to largazole thiol.

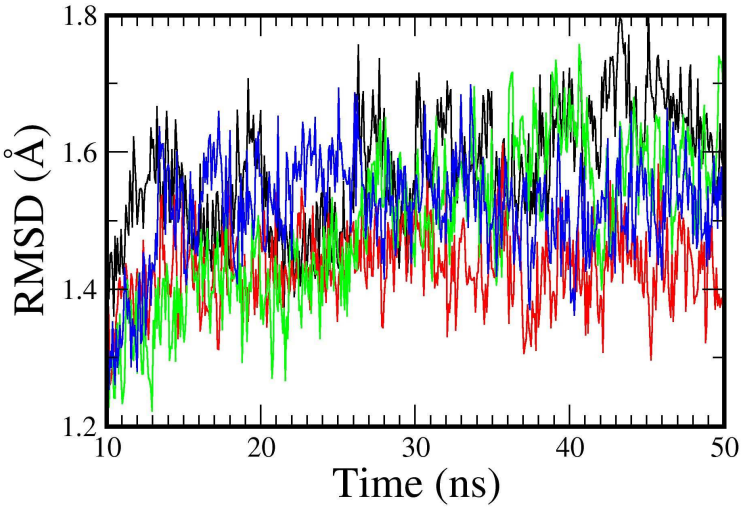

Figure 9. The root mean square deviations (A) calculated from the last 40 ns of each MD trajectory (HDAC1/largazole thiol – black; HDAC2/largazole thiol – green; HDAC1/ **7**-thiol – red; HDAC2/ **7**-thiol - blue).

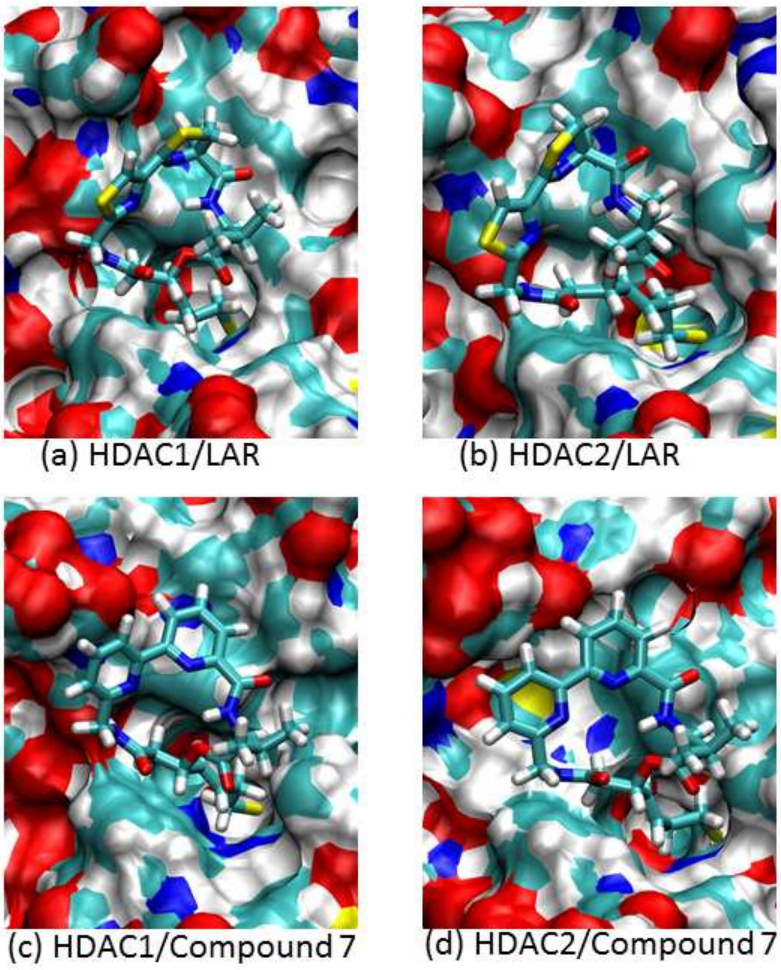

Figure 10. Snapshots representing typical configurations of (a) and (c) largazole thiol and (b) and (d) **7**-thiol bound to HDAC-1 and HDAC-2, respectively from molecular dynamics simulations. Initial structures of HDAC1 and HDAC2 used in MD were from pdb IDs 4BKX and 4IY1, respectively.

Table 3. HDAC residues that are in contacts with the ligands.

Protein	**Ligand**	**Protein residues that are in contact with the ligand**
HDAC-1	largazole	H28 P29 E98 D99 H141 G149 F150 H178 F205 D264 L271 G301 Y303
HDAC-1	Analogue **7**	H28 P29 E98 D99 H141 G149 F150 H178 F205 D264 L271 G301 Y303
HDAC-2	largazole	H33 P34 D104 H146 G154 F155 H183 F210 D269 L276 G306 Y308
HDAC-2	Analogue **7**	H33 P34 D104 H146 G154 F155 H183 F210 D269 L276 G306 Y308
HDAC-8*	largazole	K33 Y100 D101 H143 G151 F152 H180 F208 D267 M274 G304 Y306

*from reference 28.

Table 4. Enthalpies of binding (in kcal/mol) of largazole thiol and **7**-thiol bound to HDAC-1 and HDAC-2 calculated from the four simulations described in the method.

Ligand	**In HDAC-1**	**In HDAC-2**	**In solution (interaction energy with water)**
Largazole thiol	251.1 ± 7.8	252.7 ± 8.1	248.1 ± 13.0
7-thiol	256.2 ± 13.2	255.7 ± 10.2	250.1 ± 10.7

DISCUSSION

Targeting aberrant epigenetic gene silencing has gained broad recognition as a promising approach to cancer treatment.[5] The approval of four HDAC inhibitors as anticancer drugs within the last decade, the last two of which were approved within the last two years, underscores the great potential that HDAC inhibitors hold as new cancer therapeutics. Eighteen different isoforms of HDAC have been identified.[15] Of the four HDAC inhibitors approved as anticancer drugs by the FDA, SAHA, belinostat, and panobinostat target HDACs in class 1 and 2, while FK228 is a class I-selective HDAC inhibitor. HDAC inhibitors targeted to specific HDAC isoforms that are overexpressed in different forms of cancer could be useful as effective anticancer agents with minimal of undesirable side effects compared their non-selective counterparts. Although the high sequence homology present in the vicinity of the active site Zn^{2+} ion in different HDAC isoforms may not augur well for altering the zinc-binding domain of HDAC inhibitors to achieve isoform selectivity,[6,23,50] the 14 Å internal cavity near the active site constituting the acetate release channel has been explored for this purpose.[51,52] In contrast, the differences in sequence homology in the hydrophobic rim at the entrance to the active site may offer a site for exploitation to develop isoform-selective HDAC inhibitors. In this context, the class I selectivity of romidepsin may be due to the ability of its large depsipeptide ring to reach and interact with less conserved regions located further away than those accessible to smaller head groups of pan-HDAC inhibitors like vorinostat and belinostat. The depsipeptide ring of largazole may therefore be considered a viable target for chemical modification to develop isoform-selective HDAC inhibitors as well as to develop analogues with enhanced pharmacological effects.[23] Several groups,[30,32,45] including ours,[27,28] have previously reported analogues of varying levels of activity generated by altering the western half of the depsipeptide

ring. Alterations in the thiazole-thiazoline moiety constituting the eastern half of the ring have resulted in HDAC inhibitors with promising antiproliferative activity. In fact, the analogue in which the thiazole ring of largazole was replaced with a pyridine ring is a potent HDAC inhibitor.[32] In this study we made radical changes in this part of the depsipeptide ring, while maintaining the 16-membered ring size. Analogue **6** incorporated a major structural change in the depsipeptide ring with the rigid thiazole-thiazoline moiety being replaced with a more flexible and more hydrophilic polyether chain. In **7**, the thiazole-thiazoline moiety was replaced with a bi-pyridine unit, which was accompanied by a change in the hybridization at C-7 from sp^3 to sp^2. Likewise, the thiazole ring of **8** was replaced with a pyridine ring, but the thiazoline ring was replaced with an N-methyl group. The sp^3 character of the C-7 center is retained in this molecule, but the sp^2 nitrogen of the thiazoline is replaced with an sp^3 nitrogen of the N-methyl group. The N-methyl group was introduced as a handle for structural modification to modulate hydrophilicity/lipophilicity in this part of the molecule (vide infra).

The three analogues **6** - **8** showed moderate to high antiproliferative activity on HCT 116 cell line and in the NCI 60 cell line assay. Analogue **7** is the most active of the three analogues, with an activity profile similar to that of largazole. It showed highly potent growth inhibition on most cell lines tested in the NCI 60 cell line assay. In the HCT 116 cell growth inhibition assay, it had a GI_{50} of 75 nM compared to a GI_{50} of 65 nM observed for largazole The slightly higher GI_{50} value observed for largazole compared to GI_{50} of 44 nM previously reported[31] may be attributed to differences in the assay conditions.. Analogues **6** and **8** were less active than largazole and analogue **7**, both on HCT 116 cells (GI_{50} of 0.75 μM and 0.8 μM, respectively) and in the NCI 60 cell line assay. They exhibited moderate inhibitory activity on some of the melanoma, renal and leukemia cancer cell lines in the NCI assay, but were less active on other

cancer cell lines. Similarly, induction of global acetylation levels of H3K9 was apparently higher at lower concentrations for **7**, versus **6** or **8**. All three analogues maintained the same Class I selectivity as largazole, although **6** and **7** displayed greater selectivity than **8**, which showed greater inhibitory activity on HDAC6 compared to **6** and **7**.

Replacing the thiazole-thiazoline moiety with a polyether chain significantly alters its hydrophobicity/hydrophilicity, while limiting the surface area available for interaction with the hydrophobic surface area of HDAC proteins. Though less active than **7**, analogue **6** displayed an overall ~60% inhibition of the growth of the 60 cell lines at 10 μM in the NCI 60 cell line assay, and interestingly, retained class I selectivity despite the reduction in hydrophobic surface area of the depsipeptide ring. This, combined with its relatively easy method of synthesis and conceivably altered pharmacokinetic properties, makes it an interesting lead molecule for further investigation.

Replacing the thiazole-thiazoline moiety with a bi-pyridine group in analogue **7** was well tolerated in the HCT 116 cell growth inhibition assay and in the NCI-60 cell line assay, where it had an activity profile similar to that of largazole. While the compound substantially inhibited the growth of most cancer cell lines in the NCI 60 cell line assay, melanoma cell lines in general and some of the renal and CNS cancer cell lines were found to be particularly sensitive to this compound in the dose response assay. A pyridyl analogue formed by replacing the thiazole ring of largazole with a pyridine ring has previously been shown to have enhanced in vitro HDAC inhibitory activity.[32] The replacement of the thiazoline ring of largazole with a planar thiazole ring with an sp^2 C-7 center has been shown to result in reduced activity.[32] Perhaps, influenced by this observation, most largazole analogues reported to date retain the thiazoline ring at this position. In this context it is interesting to note that the replacement of the thiazoline ring with a

planar pyridine ring with an sp^2 center at C-7 in **7** had no detrimental effect on activity, although this change enforces significant conformational change in the macrocyle. It is significant that the elimination of a chiral center of unnatural amino acid (R)-α-methylcysteine origin renders bipyridyl analogues more amenable to chemical synthesis as potential anticancer agents.

Analogue **8**, although less active than analogue **7** and largazole, it too displayed an overall ~60% inhibition of the growth of the 60 cell lines at 10 μM. While it contains a pyridine ring instead of the thiazole, the thiazoline moiety was replaced with a less hydrophobic and less planar N-methyl group. In addition to the change in hybridization of the nitrogen atom from sp^2 to sp^3, this structural change also involved loss of hydrophobicity in this region of the molecule. To delineate these effects, the methyl group provides a convenient handle for chemical modification to modulate hydrophobicity in this part of the molecule and study its effect on activity. The benzyl amine analogue **9** was designed to reintroduce some degree of hydrophobicity at this position. As a further extension of this study, analogues **10** – **13** with electron withdrawing trifluoromethyl, electron donating methoxy, a hydrophobic *p*-chloro, and hydrophobic and bulky 1-naphthyl group, respectively, were designed to investigate the effect of altering electronic and steric properties at this position.

Although the replacement of the thiazole-thiazoline moiety in largazole with a flexible polyether moiety in **6** caused a reduction in cytotoxicity, there was no significant change in isoform selectivity. Interestingly, replacement of this moiety with a bi-pyridine moiety in **7** resulted in high isoform selectivity with at least 464-fold preference for class I HDAC proteins compared to class II HDAC6 protein. The class-I selectivity of **7** was even greater than that of largazole, which showed only 22-fold preference for class I. In contrast, replacement of the thiazoline ring with an N-methyl group in **8**, though not well tolerated in cytotoxicity assay,

resulted in a modest increase in inhibitory activity on HDAC6, and therefore, reduced selectivity. If the reduced hydrophobicity accompanying this structural modification is responsible for the observed reduction in isoform sensitivity, we thought that reintroducing hydrophobicity at this position may help to restore selectivity. The methyl amine group provided an appropriate handle for making such modifications and with this in mind we synthesized the benzyl analogues **9-12** and the naphthyl analogue **13**. However, such a trend was not observed in the growth inhibition activity and HDAC enzyme inhibition assay of these compounds. Although going from N-methyl to N-benzyl group caused a several fold increase in cell proliferation inhibition activity, the presence of an electron withdrawing trifluoromethyl group or an electron donating methoxy group at the para position of the benzyl group had no effect on activity. However, the introduction of a bulky and hydrophobic chlorine atom at this position caused a significant decrease in activity, which became even more pronounced when the phenyl group of the benzylamine moiety was replaced with a bulkier and more hydrophobic naphthyl group.

The great promise that largazole and analogues hold as potential clinical candidates has stimulated extensive research in their preclinical studies. Metabolism studies have shown that largazole is rapidly converted to the active metabolite largazole thiol by mouse serum and mouse microsomal proteins and by cellular proteins.[45,53] Structure-activity relationship studies have shown that the largazole macrocyle is a versatile scaffold for structural alteration to improve in vitro and in vivo potency. The analogues we synthesized provide new directions in the structural manipulation of this moiety in the development of new drug candidates.

CONCLUSION

We have prepared several analogues of the natural product largazole by structural modification of the depsipeptide ring. The replacement of the thiazole-thiazoline group of largazole with a simple polyether moiety in **6** resulted in a decrease in activity. However, the molecule still retained moderate activity on some cell lines, and given its simpler method of synthesis, it may still serve as a useful HDAC inhibitor tool and lead molecule for further structural optimization. Replacement of the thiazoline ring with an N-methyl group in **8** was also detrimental. However, this molecule retained moderate activity in some cell lines. This compound was used as a lead molecule for further structural optimization by substitution at the N-methyl handle with groups of varying degree of electronic, steric and hydrophobic/hydrophilic properties. While **6** and **8** showed moderate cell growth inhibition at the NCI-60 cell line assay, both showing ~60% overall inhibition of cells at 10 μM, analogue **7** was the most active of the three analogues. It was lethal to many of the cell lines tested in the NCI 60 cell line screen. While **6** and **8** exhibited low micromolar to mid-nanomolar GI_{50} in the dose response assay, **7** displayed low nanomolar GI_{50} values on most of the cell lines with an activity profile similar to that of largazole. It was about 400-fold more selective for Class I HDACs as compared to largazole. Given its simpler structure due to the elimination of a chiral center and its higher class I selectivity, it provides a potential drug candidate that warrants further investigation. It is to be noted that initial acute toxicity studies in the NCI Developmental Therapeutics Program showed that the compound is well tolerated in-vivo at the maximum dose of 50 mg/kg tested. It has been selected for further in vivo testing.

EXPERIMENTAL SECTION

Material and Instrumentation:

All chemicals and solvents were purchased from commercial suppliers and used without further purification, unless stated otherwise. Anhydrous THF and ether were freshly distilled from sodium and benzophenone before use. ^{1}H and ^{13}C NMR spectra were recorded on INOVA 600 MHz and Varian VXRS 400 MHz NMR spectrometers in either deuterated chloroform or deuterated methanol using residual undeuterated solvent as internal standard. HRMS were recorded on a Micromass Q-Tof II electrospray mass spectrometer at the Mass Spectrometry and Proteomics Facility, The Ohio State University, Columbus, Ohio. Melting points were determined using a Fisher-Johns melting point apparatus. Flash chromatography was performed on silica gel (40-63 μ) from Sorbent Technologies and on a Teledyne ISCO CombiFlash Companion chromatography system on RediSep prepacked silica cartridges. Uniplates (1000 μm) purchased from Analtech Inc. were used for preparative thin layer chromatography. A Waters 1525 binary pump HPLC system with Waters 2487 dual wavelength absorbance detector on a symmetry C_{18} column (5μ, 4.6 mm x 150 m)) using a linear gradient of 10 -100% H_2O/acetonitrile over 15 - 20 min; flow rate of 1 mL/min and UV detection at 211 nm and 254 nm was used for HPLC analysis. Structural integrity and purity of the test compounds were determined by the composite of ^{1}H and ^{13}C NMR, HRMS and HPLC, and all compounds were found to be >95% pure, except for compound **76** which was 91% pure.

Synthesis

Synthesis of Analogue 6

To a solution of cyclized compound **75** (40 mg, 0.076 mmol, 1 equiv) and triisopropylsilane (18 mg, 0.114 mmol, 1.5 equiv) in dichloromethane (3 mL) at 0 ^{o}C was added trifluoroacetic acid (0.26 g, 2.28 mmol, 30 equiv). The reaction mixture was stirred for 4 h at room temperature. It was concentrated in *vacuo* and the residue was dried azeotropically with toluene, and used in the next step without additional purification.

To a stirred solution of the above crude thiol (0.076 mmol, 1 equiv) and catalytic DMAP (3.0 mg) in dichloromethane (4 mL) at 0 ^{o}C were added Hunig's base (30 mg, 0.228 mmol, 3 equiv) and octanoyl chloride (31 mg, 0.19 mmol, 2.5 equiv). The reaction mixture was stirred at room temperature overnight. It was concentrated in *vacuo* and purified by flash chromatography on silica gel in 20-50% acetone/hexanes to give product **6** as a colorless oil (33mg, 83%). $[\alpha]_D^{22}$ + 13.6 (*c* 0.06, $CHCl_3$). **^{1}H NMR** (600 MHz, $CDCl_3$) δ 0.88-0.92 (dd, *J* = 14.0, 7.4 Hz, 5H), 0.96-.097 (d, *J* = 6.9 Hz, 3H), 1.28-1.32 (m, 8H), 1.64-1.68 (quin, *J* = 7.4 Hz, 2H), 1.75 (brs, 1H), 2.29-2.32 (q, 7.4 Hz, 2H), 2.32-2.38 (m, 1H), 2.52-2.60 (m, 4H), 2.90-2.92 (t, *J* = 7.3 Hz, 2H), 3.32-3.38 (m, 1H), 3.53-3.57 (m, 2H), 3.66-3.68 (m, 1H), 3.71-3.80 (m, 4H), 3.97-4.00 (d, *J* = 16.5 Hz, 1H), 4.21-4.24 (d, *J* = 17.0 Hz, 1H), 4.82-4.85 (dd, *J* = 10.3, 4.4 Hz, 1H), 5.48-5.52 (dd, *J* = 15.4, 6.6 Hz, 1H), 5.57-5.60 (m, 1H), 5.76-5.81 (dt, *J* = 15.5, 6.6 Hz, 1H), 6.13 (m, 1H), 7.33-7.35 (d, *J* = 10.3 Hz, 1H). **^{13}C NMR** (150 MHz, $CDCl_3$): δ 14.1, 17.2, 19.2, 22.6, 25.7, 27.8, 28.9, 31.6, 31.9, 32.2, 39.0, 42.1, 44.2, 56.6, 68.8, 69.2, 70.0, 71.26, 72.8, 128.7, 132.7, 169.3, 169.4, 169.7, 199.4 ppm. **HRMS**: (ESI) calcd for $C_{26}H_{44}N_2O_7S$ $[M + Na]^+$ 551.2767; found 551.2785, Anal. ($C_{26}H_{44}N_2O_7S$ - 0.3 H_2O) C, H, N.

Synthesis of Analogue 7

To a solution of the cyclized product **76** (23 mg, 0.032 mmol, 1 equiv) and triisopropylsilane (8 mg, 0.048 mmol, 1.5 equiv) in dichloromethane (2 mL) at 0 ^{o}C was added trifluoroacetic acid (0.11 g, 0.96 mmol, 30 equiv). The reaction mixture was stirred overnight at room temperature and the solvent was removed under reduced pressure. The residue was dried azeotropically with toluene, and used in the next step without additional purification.

To a stirred solution of the above crude thiol (0.032 mmol, 1 equiv) and DMAP (1.0 mg) in dichloromethane (2 mL) at 0 ^{o}C was added Hunig's base (13 mg, 0.096 mmol, 3 equiv) and octanoyl chloride (13 mg, 0.08 mmol, 2.5 equiv). The reaction mixture was stirred at room temperature overnight. It was concentrated in *vacuo*, and purified by flash chromatography on silica gel in 20-50% acetone/hexanes to give product **7** as a colorless oil (12 mg, 65%). $[\alpha]_D^{22}$ + 6.7 (*c* 0.004, $CHCl_3$). **^{1}H NMR** (600 MHz, $CDCl_3$) δ 0.88-0.90 (t, *J* = 7.1 Hz, 3H), 1.03-1.04 (d, *J* = 6.8 Hz, 3H), 1.06-1.07 (d, *J* = 6.8 Hz, 3H), 1.24-1.34 (m, 8H), 1.56-1.59 (quin, *J* = 7.1 Hz, 2H), 1.75 (m, 3H), 1.99-2.09 (m, 2H), 2.39-2.45 (m, 4H), 2.46-2.51 (m, 1H), 2.86-2.87 (d, *J* = 4.6 Hz, 2H). **^{13}C NMR** (150 MHz, $CDCl_3$): δ 14.1, 17.7, 19.1, 22.6, 25.6, 27.6, 28.9, 31.6, 32.1, 33.0, 41.6, 44.0, 44.6 58.0, 70.5, 76.8, 77.0, 77.3, 119.8, 121.4, 122.1, 123.1, 127.3, 131.5, 137.7, 138.8, 149.4, 153.2, 153.3, 156.1, 163.6, 169.0, 169.2, 199.1 ppm. **HRMS**: (ESI) calcd for $C_{43}H_{42}N_4O_4S$ $[M + Na]^+$ 617.2774; found 617.2775.

Synthesis of Analogue 8

To a solution of the cyclized product **77** (15 mg, 0.022 mmol, 1 equiv) and triisopropylsilane (6 mg, 0.033 mmol, 1.5 equiv) in dichloromethane (2 mL) at 0 ^{o}C was added trifluoroacetic acid (0.08 g, 0.66 mmol, 30 equiv). The reaction mixture was stirred for 4 h at room temperature. It was concentrated in *vacuo*, dried azeotropically with toluene, and used in the next step.

To a stirred mixture of the above obtained crude thiol and DMAP (1.0 mg) in dichloromethane (2 mL) at 0 ^{o}C was added Hunig's base (9 mg, 0.066 mmol, 3 equiv) and octanoyl chloride (9 mg, 0.055 mmol, 2.5 equiv). The reaction mixture was stirred at room temperature overnight. It was concentrated in *vacuo* and purified by flash chromatography on silica gel in 20-50% acetone/hexanes to give product **8** as colorless oil (5 mg, 41%). $[\alpha]_D^{22}$ – 7.4 (*c* 0.002, $CHCl_3$). **^{1}H NMR** (600 MHz, $CDCl_3$) δ 0.78-0.79 (d, *J* = 6.8 Hz, 3H), 0.88-0.90 (m, 6H), 1.28-1.32 (m, 8H), 1.62-1.66 (m, 2H), 2.24-2.30 (m, 3H), 2.38 (s, 3H), 2.50-2.53 (t, *J* = 7.6 Hz, 2H), 2.66-2.70 (m, 1H), 2.76-2.2.85 (m, 3H), 3.28-3.31 (d, *J* = 15.0 Hz, 1H), 3.39-3.41 (d, *J* = 16.8 Hz, 1H), 3.58-3.60 (d, *J* = 13.6 Hz, 1H), 3.86-3.88 (d, *J* = 13.6 Hz, 1H), 4.55-4.64 (dq, *J* = 17.1, 4.2 Hz, 2H), 4.85-4.87 (dd, *J* = 10.1, 4.4 Hz, 1H), 5.51-5.55 (dd, *J* = 15.6, 6.1 Hz, 1H), 5.66 (m, 1H), 5.79-5.83 (dt, *J* = 15.6, 6.8 Hz, 1H), 7.12-7.14 (d, *J* = 7.5 Hz, 1H), 7.18-7.19 (d, *J* = 7.7 Hz, 1H), 7.42 (s, 1H), 7.66-7.69 (t, *J* = 7.7 Hz, 1H), 8.68-8.70 (d, *J* = 10.1 Hz, 1H). **^{13}C NMR** (150 MHz, $CDCl_3$): δ 14.1, 17.4, 19.1, 22.6, 25.6, 27.8, 28.9, 31.6, 32.3, 32.5, 41.8, 42.8, 44.1, 44.3, 57.1, 61.1, 62.9, 72.0, 121.2, 122.1, 128.0, 132.3, 137.4, 155.6, 157.3, 169.1, 169.3, 170.4, 199.3 ppm. **HRMS**: (ESI) calcd for $C_{30}H_{46}N_4O_5S$ $[M + H]^+$ 575.3189; found 375.3198.

(*R*)-((*S*,*E*)-3,12-dioxo-2,5,8-trioxa-11-azaocta-7-(tritylthio)dec-15-en-14-yl) 2-(((9H-fluoren-9-yl)methoxy)carbonylamino)-3-methylbutanoate (14)

To a solution of Fmoc-L-valine (117 mg, 0.346 mmol, 2 equiv) in THF (1 mL) at 0 ^{o}C was added Hunig's base (67 mg, 0.519 mmol, 3 equiv) and 2,4,6-tricholorobenzoyl chloride (89 mg, 0.363 mmol, 2.1 equiv). The reaction mixture was stirred for 1 h at 0 ^{o}C. When TLC showed the formation of anhydride (100 mg, 0.173 mmol, 1 equiv), alcohol **67** and DMAP (22 mg, 0.173 mmol, 1 equiv) in THF (2 mL) were added to the reaction mixture at 0 ^{o}C. The reaction mixture

was stirred at room temperature overnight, concentrated in *vacuo*, and purified by flash chromatography on silica gel in ethyl acetate/hexanes (50-70%). The product was subjected to a second purification by reversed phase chromatography on C_{18} in acetonitrile/water (40-100%) to get **14** as a yellow oil (150 mg, 96%). $[\alpha]_D^{22}$ – 12.5 (*c* 0.7, $CHCl_3$). **^{1}H NMR** (600 MHz, $CDCl_3$) δ 0.81-0.82 (d, *J* = 6.6 Hz, 3H), 0.90-0.91 (d, *J* = 6.8 Hz, 3H), 2.03-2.06 (m, 2H), 2.10-2.18 (m, 3H), 2.45-2.49 (m, 1H), 252.-2.55 (m, 1H), 3.33-3.42 (m, 2H), 3.46-3.51 (m, 2H), 3.57-3.58 (m, 2H), 3.62-3.63 (m, 2H), 3.69 (s, 3H), 4.09 (s, 2H), 4.2-4.23 (m, 2H). 436.-4.41 (m, 2H), 5.37-5.41 (dd, *J* = 15.7, 7.5 Hz, 1H), 5,45-5.47 (d, *J* = 6.3 Hz, 1H), 5.62-5.68 (m, 2H), 6.41 (brs, 1H), 7.18-7.20 (t, *J* = 7.1 Hz, 3H), 7.25-7.28 (t, *J* = 7.8 Hz, 6H), 7.29-7.31 (t, *J* = 7.3 Hz, 2H), 7.38-7.39 (d, *J* = 7.8 Hz, 8H), 7.59-7.60 (d, *J* = 7.3 Hz, 2H), 7.74-7.76 (d, *J* = 7.3 Hz, 2H). **^{13}C NMR** (150 MHz, $CDCl_3$): δ 17.7, 19.3, 31.4, 31.6, 39.4, 41.8, 47.4, 52.1, 59.2, 66.8, 67.1, 68.6, 69.9, 70.2, 71.2, 72.8, 120.2, 120.2, 125.3, 125.3, 126.7, 127.3, 127.4, 128.0, 128.1, 128.2, 129.8, 133.9, 141.5, 141.5, 144.0, 144.1, 145.1, 156.5, 169.1, 171.1 ppm. **HRMS**: (ESI) calcd for $C_{53}H_{58}N_2O_2S$ $[M + Na]^+$ 921.3761; found 921.3752.

Methyl 6'-((5*R*,8*S*)-1-(9H-fluoren-9-yl)-5-isopropyl-3,6,10-trioxo-8-((*E*)-4-(tritylthio)but-1-enyl)-2,7-dioxa-4,11-diazadodecan-12-yl)-2,2'-bipyridine-6-carboxylate (15)

To a solution of Fmoc-L-valine (408 mg, 1.2 mmol, 2 equiv) in THF (5 mL) at 0 ^{o}C was added Hunig's base (234 mg, 1.8 mmol, 3 equiv) and 2,4,6-tricholorobenzoyl chloride (320 mg, 1.3 mmol, 2.1 equiv). The reaction mixture was stirred for 1 h at 0 ^{o}C. When TLC showed the formation of anhydride, a solution of alcohol **68** (387 mg, 0.6 mmol, 1 equiv) and DMAP (74 mg, 0.6 mmol, 1equiv) in THF (8 mL) was added to the reaction mixture at 0 ^{o}C. The reaction mixture was stirred at room temperature overnight, concentrated in *vacuo*, and purified by flash

chromatography on silica gel in ethyl acetate/hexanes (50-70%), followed by a second purification by reversed phase chromatography on C_{18} in acetonitrile/water (40-100%) to get **15** as a yellow oil (530 mg, 92%). $[\alpha]_D^{22}$ + 8.6 (*c* 0.08, $CHCl_3$). **^{1}H NMR** (600 MHz, $CDCl_3$) δ 0.84-0.85 (d, *J* = 6.8 Hz, 3H), 0.91-0.92 (d, *J* = 6.8 Hz, 3H), 2.06-2.12 (m, 2H), 2.17-2.24 (m, 2H), 2.64-2.67 (dd, *J* = 14.7, 6.3 Hz, 1H), 2.70-2.74 (dd, *J* = 14.5, 7.3 Hz, 1H), 4.04 (s, 1H), 4.18-4.21 (m, 2H), 4.30-4.32 (dd, *J* = 10.4, 7.0 Hz, 1H), 4.36-4.39 (dd, *J* = 10.3, 7.3 Hz, 1H), 4.63 (d, *J* = 5.1 Hz, 1H), 5.44-5.46 (m, 1H), 5.38-5.51 (dd, *J* = 15.2, 7.5 Hz, 1H), 5.71-5.76 (m, 2H), 7.09 (m, 1H), 7.21-7.24 (t, *J* = 7.4 Hz, 3H), 7.25-7.26 (d, *J* = 7.7 Hz, 1H), 7.28-7.32 (m, 8H), 7.38-7.40 (dd, *J* = 7.4, 3.1 Hz, 2H), 7.42-7.43 (d, *J* = 7.0 Hz, 6H), 7.57-7.59 (dd, *J* = 7.1, 4.4 Hz, 2H), 7.75-7.78 (t, *J* = 7.7 Hz, 3H), 7.90-7.92 (t, *J* = 7.7 Hz, 1H), 8.12-8.13 (d, *J* = 6.7 Hz, 1H), 8.41-8.42 (d, *J* = 7.7 Hz, 1H), 8.56-8.58 (d, *J* = 7.9 Hz, 1H). **HRMS**: (ESI) calcd for $C_{59}H_{56}N_4O_7S$ $[M + Na]^+$ 987.3789; found 987.3705.

(*R*)-((*S*,*E*)-1-((6-(((2-methoxy-2-oxoethyl)(methyl)amino)methyl)pyridin-2-yl)methylamino)-1-oxo-7-(tritylthio)hept-4-en-3-yl) 2-(((9H-fluoren-9-yl)methoxy)carbonylamino)-3-methylbutanoate (16)

To a solution of Fmoc-L-valine (1.40 g, 4.2 mmol, 2 equiv) in THF (15 mL) at 0 ^oC was added Hunig's base (0.82 g, 6.3 mmol, 3 equiv) and 2,4,6-tricholorobenzoyl chloride (1.1 g, 4.6 mmol, 2.1 equiv). The reaction mixture was stirred for 1 h at 0 ^oC. When TLC showed the formation of the anhydride product, a solution of alcohol **69** (1.31 g, 2.1 mmol, 1 equiv) and DMAP (0.26 g, 2.1 mmol, 1equiv) in THF (20 mL) were added to the reaction mixture at 0 ^oC. The reaction mixture was stirred at room temperature overnight, concentrated in *vacuo* and purified by flash chromatography on silica gel in dichloromethane/ethyl acetate (20-50%), followed by a second purification by reversed phase chromatography on C_{18} in acetonitrile/water (40-100%) to get **16**

as a yellow oil (1.8 g, 90%). $[\alpha]_D^{22} = -5.5$ (*c* 0.04, $CHCl_3$). **^{1}H NMR** (600 MHz, $CDCl_3$) δ 0.83-0.84 (d, *J* = 6.7 Hz, 3H), 0.91-0.93 (d, *J* = 6.8 Hz, 1H), 2.05-2.09 (m, 2H), 2.11-2.14 (q, *J* = 6.5 Hz, 1H), 2.192-.22 (m, 2H), 2.44 (s, 3H), 2.57-2.60 (dd, *J* = 15.7, 5.1 Hz, 1H), 2.66-2.69 (dd, *J* = 14.5, 7.5 Hz, 1H), 3.36 (s, 2H), 3.72 (s, 3H), 3.83 (s, 2H), 4.20-4.23 (m, 2H), 4.32-4.35 (m 1H), 4.37-4.40 (m, 1H), 4.51-4.52 (t, *J* = 4.8 Hz, 2H), 5.38-5.40 (d, *J* = 8.6 Hz, 1H), 5.43-5.47 (dd, *J* = 15.2, 7.4 Hz, 1H), 5.69-5.72 (m, 2H), 6.98 (m, 1H), 7.08-7.09 (d, *J* = 7.5 Hz, 1H), 7.21-7.23 (t, *J* = 7.3 Hz, 3H), 7.28-7.30 (t, *J* = 7.9 Hz, 6H), 7.32-7.34 (t, *J* =7.3 Hz, 3H), 7.40-7.43 (m, 9H), 7.59-7.62 (m, 3H), 7.77-7.78 (d, *J* = 7.5 Hz, 2H). **^{13}C NMR** (150 MHz, $CDCl_3$): δ 17.5, 19.0, 31.2, 31.3, 31.4, 41.6, 42.7, 44.5, 47.2, 51.6, 57.9, 59.0, 62.4, 66.6, 67.0, 72.6, 120.0, 120.0, 120.4, 121.8, 125.1, 126.6, 127.1, 127.7, 127.9, 128.0, 129.6, 133.8, 137.3, 141.3, 143.8, 143.9, 144.8, 155.7, 156.2, 157.8, 168.7, 171.0, 171.4 ppm. **HRMS**: (ESI) calcd for $C_{57}H_{60}N_4O_7S$ $[M + H]^+$ 945.4261; found 945.4244.

Methyl 6'-(aminomethyl)-2,2'-bipyridine-6-carboxylate (23)

To a mixture of nitrile **50** (720 mg, 3 mmol) in MeOH (15 mL) and trifluoroacetic acid (1 mL) was added 5% Pd/C (70 mg, 5 wt%). The reaction mixture was stirred under hydrogen at 3 atm for 6 h. After disappearance of starting material (TLC), the reaction mixture was filtered through a pad of celite to remove palladium catalyst, concentrated under reduced pressure. The product **23** was used in the next step with no further purification.

General procedure for reduction (hydrogenation) of azide to the corresponding primary amine (24-27)

A mixture of azide **61-64** (3 mmol) dissolved in MeOH (15 mL) and 5% Pd/C (10 wt. %) was stirred under hydrogen at 3 atm for 6-8 h. After disappearance of starting material (TLC), the reaction mixture was filtered through a pad of celite, concentrated in *vacuo* and used in the next step without further purification.

(*S*,*E*)-3-Hydroxy-1-((*R*)-4-isopropyl-2-thioxothiazolidin-3-yl)-7-(tritylthio)hept-4-en-1-one (30)

To a stirred solution of acetyl Nagao **32** (1.493 g, 7.355 mmol, 1 equiv) in dichloromethane (60 mL) at 0 ^{o}C, was added $TiCl_4$ (1.72 g, 9.05 mmol, 1.23 equiv). After stirring for 5 minutes at 0 ^{o}C the reaction mixture was cooled to -78 ^{o}C and Hunig's base (1.872 g, 9.02 mmol, 1.25 equiv) was added. The reaction mixture was stirred for 2 h at -78 ^{o}C and the aldehyde **33** (2.6 g, 7.26 mmol, 0.987 equiv) in dichloromethane (8 mL) was added dropwise. The reaction mixture was stirred for 1 h at -78 ^{o}C, treated with water (15 mL), and diluted with dichloromethane (50 mL). The layers were separated and the aqueous layer was extracted with dichloromethane. The combined organic extract was washed with saturated NaCl (40 mL) and dried over anhydrous sodium sulfate. The solvent was removed in *vacuo* and the residue was purified by flash chromatography on silica gel in dichloromethane/hexanes (25-90%) to give the major isomer **30** as a yellow oil (3.5 g, 86%). $[\alpha]_D^{20}$ – 138.0 (*c* 1.0, $CHCl_3$). **^{1}H NMR** (600 MHz, $CDCl_3$) δ 0.97-0.99 (d, *J* = 6.9 Hz, 1H), 1.05-1.07 (d, *J* = 7.0 Hz, 1H), 2.06-2.13 (m, 2H), 2.21-2.25 (t, *J* = 7.0 Hz, 2H), 2.32-2.40 (m, 1H), 2.88 (brs, 1H), 2.962-.99 (d. *J* = 11.7 Hz, 1H), 3.27-3.33 (dd, *J* = 17.6, 8.7 Hz, 1H), 3.43-3.48 (dd, *J* = 11.3, 8.0 Hz, 1H), 3.55-3.60 (dd, *J* = 17.5, 2.5 Hz, 1H), 4.57-4.58 (m, 1H), 5.11-5.15 (t, *J* = 7.0 Hz, 1H), 5.45-5.50 (dd, *J* = 15.4, 5.9 Hz, 1H), 5.57-5.64

(m, 1H), 7.207.23 (t, *J* = 7.3 Hz, 3H), 7.27-7.31 (t, *J* = 8.0 Hz, 5H), 7.42-7.44 (d, *J* = 7.6 Hz, 7H). **^{13}C NMR** (150 MHz, $CDCl_3$): δ 18.1, 19.4, 30.9, 31.1, 31.7, 31.7, 45.6, 66.8, 68.7, 71.7, 126.9, 128.1, 129.8, 130.2, 132.2, 145.1, 172.7, 203.2 ppm.

(*E*)-5-(Tritylthio)pent-2-enal (33)

To a solution of nitrile **38** (355 mg, 1 mmol, 1 equiv) in toluene (5 mL) at -78 ^{o}C was added DIBAL-H (1.33 mL of 1.2 M solution in hexanes, 1.5 mmol, 1.5 equiv). The reaction mixture was stirred for 3 h at -78 ^{o}C and allowed to warm to room temperature. Water (10 mL) was added and the mixture was stirred for 15 min. It was extracted with ether (3 x 20 mL), washed with brine, and dried over anhydrous sodium sulfate. The solvent was removed under reduced pressure and the crude product was purified by passing through a silica plug in dichloromethane to afford aldehyde **33** as white crystals (322 mg, 90%). mp 144-148 ^{o}C. **^{1}H NMR** (600 MHz, $CDCl_3$) δ 2.27-2.31 (m, 2H), 2.34-2.36 (t, *J* = 6.9 Hz, 2H), 5.96-6.00 (q, *J* = 7.8 Hz, 1H), 6.60-6.64 (dt, *J* = 15.7, 6.5 Hz, 1H), 7.21-7.25 (t, *J* = 7.4, Hz, 3H), 7.28-7.30 (t, *J* = 7.8 Hz, 6H), 7.42-7.43 (d, *J* = 8.0 Hz, 6H). **^{13}C NMR** (100 MHz, $CDCl_3$): δ 30.24, 31.96, 67.22, 127.03, 128.23, 129.76, 133.85, 144.79, 156.09, 149.03 ppm.

3-(Tritylthio)propanal (36)

To a solution of triphenylmethanethiol (1.38 g, 5 mmol, 1 equiv) in dichloromethane (20 mL) was added acrolein (0.393 g, 7 mmol, 1.4 equiv) and triethylamine (0.71 g, 7 mmol, 1.4 equiv). The reaction mixture was stirred for 1 h at room temperature and was concentrated under reduced pressure to give aldehyde **36** as an off-white solid (1.66 g, 99%). mp 98-99 ^{o}C. **^{1}H NMR**

(600 MHz, $CDCl_3$) δ 2.35-2.39 (t, *J* = 7.3 Hz, 2H), 2.45-2.49 (t, *J* = 6.6 Hz, 2H), 7.21-7.24 (t, *J* = 7.3 Hz, 3H), 7.28-7.32 (t, *J* = 8.0 Hz, 5H), 7.42-7.44 (d, *J* = 7.6 Hz, 7H), 9.56 (s, 1H). **^{13}C NMR** (150 MHz, $CDCl_3$): δ 24.6, 42.9, 127.0, 128.2, 129.8, 144.7, 200.6 ppm. It was used in the next step without purification.

(*E*:*Z*)-5-(Tritylthio)pent-2-enenitrile (38)

To a suspension of (cyanomtheyl)triphenylphosphonium chloride (5.06 g, 15 mmol, 1.5 equiv) in dry dichloromethane (50 mL) was added triethylamine (3.80 g, 38 mmol, 3.9 equiv). The reaction mixture was stirred at room temperature for 45 min and the solvent was removed under reduced pressure to give (cyanomethylene)triphenylphosphorane **37** as a yellow solid, which was used in the next step without further purification.

A mixture of aldehyde **36** (3.33 g, 10 mmol, 1 equiv) and (cyanomethylene)triphenylphosphorane **37** obtained above in dry benzene (50 mL) was heated under reflux for 3 h. The reaction mixture was concentrated under reduced pressure and purified by passing through a silica plug in 50% dichloromethane/hexanes to afford *cis* : *trans* (1:3) mixture of nitrile **38** (3.2 g, 90%) as a white solid, mp 124-126 ^{o}C . It was used in the next step without further purification.

3,6,11-Trioxa-9-azatridecanoic acid, 12,12-dimethyl-10-oxo-, methyl ester (43)

To a stirred solution of 2-(2-aminoethoxy)ethanol 39 (1.05 g, 10 mmol, 1 equiv) in anhydrous ethanol (15 mL) at 0 ^{o}C was added di-*tert*-butyl dicarbonate (2.2 g, 10 mmol, 1 equiv). The

reaction mixture was stirred for 2 hours at room temperature. It was concentrated under reduced pressure, re-dissolved in dichloromethane, and washed with brine. The organic extract was dried over anhydrous sodium sulfate and the solvent was removed under reduced pressure to give the crude product as a colorless oil. The product **40** was used in the next step without further purification. **^{1}H NMR** (600 MHz, $CDCl_3$) δ 1.44 (s, 9H), 3.33-3.34 (m, 2H), 3.54-3.59 (dt, *J* = 10.4, 5.2 Hz, 2H), 3.73-3.75 (dt, *J* = 4.3, 3.4 Hz, 2H).

A mixture of methyl bromoacetate (2.0 g, 1.24 mL, 13.1 mmol, 1 equiv) and sodium iodide (2.51 g, 16.7 mmol, 1.28 equiv) in acetone (9 mL) was stirred at room temperature for 3 h. The reaction mixture was filtered and the white solid was washed with ether (3 x 5 mL). The organic extract was concentrated under reduced pressure. The residue was re-dissolved in dichloromethane, washed with brine, dried over anhydrous sodium sulfate and solvent removed under reduced pressure to give methyl iodoacetate **42** as an orange yellow oil (2.2 g, 85%).

To a stirred solution of 2-[2-(boc-amino)ethoxy]ethanol **40** (0.20 g, 1 mmol, 1 equiv) in anhydrous dimethylformamide (4 mL) at 0 ^{o}C was added sodium hydride (66 mg, of 60% dispersion in oil, 1.5 equiv). The reaction mixture was stirred for 1 h at 0 ^{o}C, and methyl iodoacetate **42** (480 mg, 2.4 mmol, 2.4 equiv) was added. The reaction mixture was stirred overnight at room temperature. After adding water, the reaction mixture was extracted with dichloromethane (2 x 10 mL). The combined organic extract was washed with water (2 x 10 mL), dried over anhydrous sodium sulfate, and the solvent evaporated under reduced pressure. The residue was purified by flash chromatography on silica gel in ethyl acetate/hexanes (5-10%) to give **43** as a yellow oil (215 mg, 78%).**^{1}H NMR** (600 MHz, $CDCl_3$) δ 1.44 (s, 9H), 3.31-3.32 (m, 2H), 3.53-3.56 (t, *J* = 5.1 Hz, 2H), 3.64-3.66 (m, 2H), 3.71-3.73 (m, 2H), 3.76 (s, 3H), 4.16

(s, 2H). **^{13}C NMR** ($CDCl_3$, 150 MHz): δ 28.7, 40.58, 52.11, 68.82, 70.52, 70.58, 71.15, 156.20, 171.05 ppm. **HRMS**: (ESI) calcd for $C_{12}H_{23}NO_6$ $[M + Na]^+$ 300.1423; found, 300.1417

6-Bromo-6'-methyl-2,2'-bipyridine (47)

To a stirred solution of 2-bromo-6-methylpyridine **44** (1.25 g, 7.3 mmol, 1 equiv) in dry ether (40 mL) at -78 ^oC was added n-butyllithium (4.6 mL, 1.6 M solution in hexanes, 7.3 mmol, 1 equiv) dropwise over a period of 10 min under nitrogen. The reaction mixture was stirred at -78 ^oC for 1 h, followed by dropwise addition of a solution of trimethyltin chloride (1.5 g, 7.5 mmol) solution in dry THF (8 mL). The reaction mixture was stirred for 3 h at room temperature, filtered through a pad of celite, and concentrated in *vacuo* to give the tin derivative 2-methyl-6-trimethylstannylpyridine **45** as yellow oil. The crude reaction product was used in the next step without additional purification.

To a mixture of 2,6-dibromopyridine **46** (1.73 g, 7.3 mmol), LiCl (1.15 g, 14.6 mmol), and $Pd(PPh_3)_4$ (0.22 g, 0.2 mmol) was added a solution of **45** (2.3 g, 7.3 mmol) in toluene (5 mL) under nitrogen atmosphere. The reaction mixture was heated under reflux at 120 ^oC for 24 h, solvent was evaporated in *vacuo*, and the residue purified by flash chromatography on silica gel in dichloromethane/hexanes (50-100%) to get **47** as a yellow powder (1.10 g, 60%). mp 138-143 ^oC. **^{1}H NMR** (600 MHz, $CDCl_3$) δ 4.04 (s, 3H), 7.52-7.54 (d, J = 7.9 Hz, 1H), 7.69-7.72 (t, J = 7.9 Hz, 1H), 7.96-7.99 (t, J = 7.9 Hz, 1H), 8.15-8.16 (d, J = 7.0 Hz, 1H), 8.52-8.53 (d, J = 7.7 Hz, 1H), 8.60-8.61 (d, J = 7.9 Hz, 1H). **^{13}C NMR** (150 MHz, $CDCl_3$): δ 53.0, 120.4, 124.7, 125.6, 128.6, 138.1, 139.4, 141.6, 147.6, 154.8, 156.3, 165.7 ppm.

6'-Bromo-2,2'-bipyridine-6-carboxylic acid (48)

A powder of 6-bromo-6'-methyl-2,2'-bipyridine **47** (1.4 g, 5.6 mmol) was added carefully and gradually over 15 min to sulfuric acid (10 mL) at 0 ^{o}C under vigorous stirring (violent exothermic acid-base reaction). Chromium (VI) oxide (1.7 g, 17 mmol) was added to the reaction mixture in 5-6 portions to maintain reaction temperature below 4 ^{o}C. The resulting thick green slurry of reaction mixture was allowed to stir overnight at room temperature. It was poured over ice cooled water, and the resulting white solid was filtered, washed with cold water and dried overnight under reduced pressure to give carboxylic acid **48** as a white solid (1.41 g, 90%), mp 248-260 ^{o}C (decomposition). **^{1}H NMR** (600 MHz, DMSO) δ 7.77-7.78 (d, *J* = 7.9 Hz, 1H), 7.96-7.99 (t, *J* = 7.9 Hz, 1H), 8.13-8.18 (m, 2H), 8.48-8.49 (dd, *J* = 7.5, 1.1 Hz, 1H), 8.55-8.57 (d, *J* = 7.7 Hz, 1H). **^{13}C NMR** (150 MHz, DMSO): δ 120.9, 124.3, 125.9, 129.4, 139.6, 141.3, 141.6, 148.6, 154.0, 156.3, 166.3 ppm.

Methyl 6'-bromo-2,2'-bipyridine-6-carboxylate (49)

A mixture of 6'-bromo-2, 2'-bipyridine-6-carboxylic acid **48** (1.11 g, 4 mmol) in methanol (15 mL) and conc. sulfuric acid (1.5 mL) was stirred at room temperature for 5 minutes. The reaction mixture was heated in a microwave synthesizer at 80 ^{o}C for 2 h. The solvent was removed under reduced pressure, and the residue was suspended in water, basified with sodium hydroxide and extracted with dichloromethane. The organic extract was washed with brine, dried over anhydrous sodium sulfate and the solvent was removed under reduced pressure. The product was purified by flash chromatography on silica gel in ethyl acetate/hexanes (10-30%) to get **49** as white a solid (1.17 g, 99%). mp 143-144 ^{o}C. **^{1}H NMR** (600 MHz, $CDCl_3$) δ 4.06 (s, 3H), 7.75-7.77 (dd, *J* = 7.7, 1.1 Hz, 1H), 8.00-8.02 (t, *J* = 8.1 Hz, 1H), 8.02-8.05 (t, *J* = 7.9 Hz, 1H), 8.20-

8.22 (dd, *J* = 7.7, 1.1 Hz, 1H), 8.67-8.68 (dd, *J* = 7.9, 1.0 Hz, 1H), 8.82-8.83 (dd, *J* = 8.2, 1.1 Hz, 1H). **^{13}C NMR** (150 MHz, $CDCl_3$,): δ 53.0, 117.3, 124.7, 124.8, 126.0, 128.6, 133.2, 138.2, 138.4, 147.7, 154.3, 156.7, 165.5 ppm. **HRMS**: (ESI) calcd for $C_{12}H_9BrN_2O_2$ $[M + Na]^+$ 314.9745; found, 314.9739.

Methyl 6'-cyano-2,2'-bipyridine-6-carboxylate (50)

To a solution of methyl 6'-bromo-2,2'-bipyridine-6-carboxylate **49** (0.673 g, 2.3 mmol, 1 equiv) in DMF (5 mL) in a microwave vial was added cuprous cyanide (0.31 g, 3.45 mmol, 1.5 equiv). The reaction mixture was heated in a microwave synthesizer at 160 ^oC for 1 h. The reaction mixture was allowed to cool to room temperature. A warm aqueous solution of potassium cyanide (0.6 g in 5 mL of water) was added, which resulted in the precipitation of a white solid. The resulting suspension was stirred for 1 h at room temperature, and extracted with ether. The combined organic extract was washed with brine, dried over anhydrous sodium sulfate, and the solvent was removed under reduced pressure. The residue was purified by flash chromatography on silica gel in dichloromethane to give **50** as a white solid (440 mg, 75%); mp 198-201 ^oC. **^{1}H NMR** (600 MHz, $CDCl_3$) δ 4.06 (s, 3H), 7.75-7.77 (dd, *J* = 7.7, 1.1 Hz, 1H), 8.00-8.02 (t, *J* = 8.1 Hz, 1H), 8.02-8.05 (t, *J* = 7.9 Hz, 1H), 8.20-8.22 (dd, *J* = 7.7, 1.1 Hz, 1H), 8.67-8.68 (dd, *J* = 7.9, 1.0 Hz, 1H), 8.82-8.83 (dd, *J* = 8.2, 1.1 Hz, 1H). **^{13}C NMR** (150 MHz, $CDCl_3$): δ 53.0, 117.3, 124.7, 124.8, 126.0, 128.6, 133.2, 138.2, 138.4, 147.7, 154.3, 156.7, 165.5 ppm. **HRMS**: (ESI) calcd for $C_{13}H_9N_3O_2$ $[M + Na]^+$ 262.0592; found, 262.0627.

(6-(Hydroxymethyl)pyridin-2-yl)methyl 4-methylbenzenesulfonate (52)

A mixture of 2,6-pyridinedimethanol **51** (1.39 g, 10 mmol, 1 equiv), silver oxide (4.00 g, 15 mmol, 1.4 equiv), and potassium iodide (0.35 g, 2 mmol, 0.2 equiv) in dichloromethane (70 mL) was cooled to -20 ^{o}C. Tosyl chloride (1.90 g, 10 mmol, 1 equiv) was added and the reaction mixture was stirred at -20 ^{o}C for 30 min. It was warmed to room temperature and stirred for an additional 3 h. The reaction mixture was filtered through a celite pad, and washed with ethyl acetate. The solvent was removed under reduced pressure and the residue was purified by flash chromatography on silica gel in dichloromethane/hexanes (20-100%) to give **52** as a pink oil (2.4 g, 82%). **^{1}H NMR** (600 MHz, $CDCl_3$) δ 2.46 (s, 3H), 4.71 (s, 2H), 5.16 (s, 2H), 7.19-7.21 (d, *J* = 7.7 Hz, 1H), 7.33-7.34 (d, *J* = 7.7 Hz, 1H), 7.35-7.37 (d, *J* = 8.1 Hz, 2H), 7.69-7.72 (t, *J* = 7.9 Hz, 1H), 7.83-7.85 (d, *J* = 6.6 Hz, 2H). **^{13}C NMR** (150 MHz, $CDCl_3$): δ 21.7, 63.8, 71.4, 120.2, 120.6, 128.1, 129.9, 132.8, 137.7, 145.1, 152.6, 158.9 ppm.

(6-(Azidomethyl)pyridin-2-yl)methanol (53)

A mixture of compound **52** (1.66 g, 5.67 mmol) and NaN_3 (1.1 g, 17.01 mmol) in DMF (40 mL) was stirred at 80 ^{o}C for 3h. The solvent was removed under reduced pressure and the residue was dissolved in ethyl acetate, filtered through a pad of celite and evaporated in *vacuo* to give **53** as a greenish solid (920 mg, 98%). **^{1}H NMR** (600 MHz, $CDCl_3$) δ 4.48 (s, 2H), 4,78 (s, 2H), 7.22-7.24 (d, *J* = 7.7 Hz, 1H), 7.25-7.26 (d, *J* = 6.5 Hz, 1H), 7.72-7.75 (t, *J* = 7.5 Hz, 1H). **^{13}C NMR** (150 MHz, $CDCl_3$): δ 55.3, 64.0, 119.7, 120.5, 137.7, 154.9, 159.3 ppm.

(6-(Azidomethyl)pyridin-2-yl)methyl 4-methylbenzenesulfonate (54)

To a mixture of compound **53** (380 mg, 2.3 mmol, 1 equiv) in THF (2 mL) and water (2 mL) at 0 ^{o}C was added NaOH (0.27 g, 6.9 mmol, 3 equiv), followed by dropwise addition of a solution of tosyl chloride (0.483 g, 2.53 mmol, 1.1 equiv) in THF (2 mL). The suspension was stirred at 0 ^{o}C for 4 h and extracted with dichloromethane. The combined organic extract was washed with brine, dried over anhydrous sodium sulfate and the solvent removed under reduced pressure to give compound **54** as a yellow oil (621 mg, 85%). **^{1}H NMR** (600 MHz, $CDCl_3$) δ 2.47 (s, 3H), 4.42 (s, 3H), 5.16 (s, 2H), 7.28-7.29 (d, *J* = 6.4 Hz, 1H), 7.36-7.37 (d, *J* = 8.4 Hz, 2H), 7.39-7.41 (d, *J* = 7.9 Hz, 1H), 7.73-7.76 (t, *J* = 7.7 Hz, 1H), 7.84-7.86 (d, *J* = 6.8 Hz, 2H). **^{13}C NMR** (150 MHz, $CDCl_3$): δ 21.7, 55.3, 71.5, 121.0, 121.5, 128.1, 129.9, 132.8, 138.0, 145.0, 153.9, 155.5 ppm.

General procedure for the secondary amine alkylation reaction (61-66).

A mixture of 2-tosylmethyl-6-azidomethylpyridine **54** (1 mmol, 1 equivalent), amine **55-58** (1 mmol, 1 equivalent), and potassium carbonate (2 mmol, 2 equivalent) in acetonitrile (10 mL) was refluxed under nitrogen for 3 h. When TLC showed disappearance of starting materials, the reaction mixture was cooled to room temperature, treated with water, and extracted three times with ethyl acetate. The organic extract was dried over anhydrous sodium sulfate, filtered and solvent removed under reduced pressure. The residue was purified by flash column chromatography on silica gel in dichloromethane/ethyl acetate (10-50%).

Methyl 2-(((6-(azidomethyl)pyridin-2-yl)methyl)(methyl)amino)acetate (61).

Yellow oil (0.20 g, 81%). **^{1}H NMR** (600 MHz, $CDCl_3$) δ 2.45 (s, 3H), 3.38 (s, 2H), 3.73 (s, 3H), 3.86 (s, 3H), 4.47 (s, 2H), 7.23-7.24 (d, *J* = 7.7 Hz, 1H), 7.44-7.45 (d, *J* = 7.7 Hz, 1H), 7.70-7.72 (t, *J* = 7.7 Hz,1H). **^{13}C NMR** (150 MHz, $CDCl_3$): δ 42.6, 51.6, 55.6, 57.9, 62.5, 120.4, 122.4, 137.5, 155.1, 158.9, 171.4 ppm. **HRMS**: (ESI) calcd for $C_{11}H_{15}N_5O_2$ $[M + Na]^+$ 272.1123; found 272.1134.

Methyl 2-(((6-(azidomethyl)pyridin-2-yl)methyl)(benzyl)amino)acetate (62).

Yellow oil (0.30 g, 86%). **^{1}H NMR** (600 MHz, $CDCl_3$) δ 3.42 (s, 2H), 3.71 (s, 3H), 3.86 (s, 2H), 3.98 (s, 2H), 4.46 (s, 2H), 7.21-7.23 (d, *J* = 7.5 Hz, 1H), 7.25-7.28 (t, *J* = 7.3 Hz, 1H), 7.32-7.35 (t, *J* = 7.7 Hz, 2H), 7.40-7.42 (d, *J* = 7.6 Hz, 1H), 7.57-7.59 (d, *J* = 7.7 Hz, 1H), 7.71-7.73 (t, *J* = 7.7 Hz, 1H). **^{13}C NMR** (150 MHz, $CDCl_3$) δ 51.5, 54.2, 55.6, 58.1, 59.6, 120.3, 122.2, 127.3, 128.4, 129.0, 137.5, 138.5, 154.9, 159.8, 171.7 ppm. **HRMS**: (ESI) calcd for $C_{17}H_{19}N_5O_2$ $[M + Na]^+$ 362.1593; found 362.1576.

Methyl 2-(((6-(azidomethyl)pyridin-2-yl)methyl)(4-methoxybenzyl)amino)acetate (63).

Yellow oil (0.25 g, 77%). **^{1}H NMR** (600 MHz, $CDCl_3$) δ 3.43 (s, 2H), 3.73 (s, 3H), 3.92 (s, 2H), 3.98 (s, 2H), 4.46 (s, 2H), 7.23-7.24 (d, *J* = 7.5 Hz, 1H), 7.51-7.52 (d, *J* = 7.7 Hz, 1H), 7.54-7.55 (d, *J* = 8.1 Hz, 2H), 7.58-7.60 (d, *J* = 8.1 Hz, 2H), 7.72-7.74 (t, *J* = 7.7 Hz, 1H). **^{13}C NMR** (150 MHz, CDCl3): δ 51.5, 54.3, 55.5, 57.7, 59.6, 120.5, 122.2, 125.1, 125.3, 125.3, 125.3, 125.3, 129.1, 129.4, 129.6, 137.6, 142.9, 155.0, 159.3, 171.5 ppm. **HRMS**: (ESI) calcd for $C_{18}H_{18}F_3N_5O_2$ $[M + Na]^+$ 416.1310; found 416.1315.

Methyl 2-(((6-(azidomethyl)pyridin-2-yl)methyl)(4-(trifluoromethyl)benzyl)amino)acetate (64).

Yellow oil (0.35 g, 89%), **^{1}H NMR** (600 MHz, $CDCl_3$) δ 3.39 (s, 2H), 3.71 (s, 3H), 3.78 (s, 2H), 3.81 (s, 3H), 3.96 (s, 2H), 4.46 (s, 2H), 6.86-6.88 (d, *J* = 8.6 Hz, 2H), 7.21-7.23 (d, *J* = 7.7 Hz, 1H), 7.31-7.32 (d, *J* = 8.6 Hz, 2H), 7.56-7.57 (d, *J* = 7.7 Hz, 1H), 7.71-7.73 (t, *J* = 7.7 Hz, 1H). **^{13}C NMR** (150 MHz, CDCl3): δ 51.5, 54.0, 55.3, 55.6, 57.5, 59.4, 113.7, 120.3, 122.2, 130.2, 130.4, 137.5, 154.8, 158.9, 159.9, 171.8 ppm. **HRMS**: (ESI) calcd for $C_{18}H_{21}N_5O_3$ $[M + Na]^+$ 373.1542; found 373.1615.

2-(Trimethylsilyl)ethyl N-((6-(azidomethyl)pyridin-2-yl)methyl)-N-(4-chlorobenzyl)glycinate (65)

Yellow oil (0.76 g, 85%). **^{1}H NMR** (600 MHz, $CDCl_3$): δ 0.04 (s, 9H), 1.00 (d, *J* = 6.7 Hz, 2H), 1.62 (s, 2H), 3.34 (s, 2H), 3.80 (s, 2H), 3.93 (s, 2H), 4.20 (d, *J* = 8.7 Hz, 2H), 4.45 (s, 2H), 7.22 (d, *J* = 7.6 Hz, 1H), 7.28 (d, *J* = 8.4 Hz, 2H), 7.34 (d, *J* = 8.4 Hz, 2H), 7.53 (d, *J* = 7.7 Hz, 1H), 7.72 (d, *J* = 7.7 Hz, 1H).

^{13}C NMR (151 MHz, $CDCl_3$): δ -1.51, 17.44, 54.48, 55.55, 57.42, 59.51, 62.77, 120.35, 122.17, 128.48, 130.30, 132.93, 137.15, 137.54, 154.94, 171.27 ppm. **HRMS**: (ESI) calcd for $C_{21}H_{28}ClN_5O_2Si$ $[M + H]^+$ 446.1779; found 446.1780.

2-(Trimethylsilyl)ethyl N-((6-(azidomethyl)pyridin-2-yl)methyl)-N-(naphthalen-1-ylmethyl)glycinate (66)

Yellow oil (0.55 g, 95%). **^{1}H NMR** (600 MHz, $CDCl_3$): δ 0.04 (s, 9H), 1.06-0.95 (d, *J* = 6.7 Hz, 2H), 3.39 (s, 2H), 4.01 (s, 2H), 3.93 (s, 2H), 4.24- 4.14 (d, *J* = 8.7 Hz, 2H), 4.32 (s, 2H), 4.44 (s, 2H), 7.17 (d, *J* = 7.6 Hz, 1H), 7.44 – 7.36 (m, 2H), 7.56 – 7.46 (m, 3H), 7.61 (t, *J* = 9.4 Hz, 1H), 7.77 (d, *J* = 8.2 Hz, 1H), 7.87 – 7.81 (d, *J*=8.2, 1H), 8.42 (d, *J* = 7.9 Hz, 1H). **^{13}C NMR** (150 MHz, $CDCl_3$): δ 1.49, 17.43, 54.90, 55.58, 56.97, 59.75, 62.71, 120.16, 122.29, 124.98, 125.20, 125.69, 125.83, 127.85, 128.27, 128.37, 132.52, 133.86, 134.17, 137.40, 154.74, 159.89, 171.52. **HRMS**: (ESI) calcd for $C_{25}H_{31}N_5O_2Si$ $[M + H]^+$ 462.2325; found 462.2336.

(*S*,*E*)-methyl 2-(2-(2-(3-hydroxy-7-(tritylthio)oct-4-enamido)ethoxy)ethoxy)acetate (67)

A solution of compound **43** (140 mg, 0.5 mmol, 1 equiv) in TFA/DCM (1:2) (7 mL) was stirred at room temperature for 2 h. The reaction mixture was concentrated under reduced pressure and the residue was dried azeotropically with toluene. To a solution of the above product **22** in dichloromethane (5 mL) was added DMAP (62 mg, 0.5 mmol, 1 equiv), and Hunig's base (130 mg, 1 mmol, 2 equiv). The reaction mixture was stirred at room temperature for 30 min, followed by addition of a solution of the aldol product **30** (280 mg, 0.5 mmol, 1 equiv) in dichloromethane (5 mL). It was stirred at room temperature overnight, concentrated in *vacuo*, and purified by flash chromatography on silica gel in ethyl acetate/hexanes (80-100%) to get **67** as a yellow oil (260 mg, 93%). $[\alpha]_D^{22}$ – 6.8 (*c* 1.0, $CHCl_3$). **^{1}H NMR** (600 MHz, $CDCl_3$) δ 2.03-2.09 (m, 2H), 2.17-2.21 (t, *J* = 7.3 Hz, 1H), 2.28-2.34 (m, 1H), 2.37-2.42 (m, 1H), 3.41-3.45 (m, 2H), 3.54-3.56 (t, *J* = 5.0 Hz, 1H), 3.63-3.71 (m, 4H), 3.70 (s, 1H), 4.01-4.02 (d, *J* = 3.3 Hz, 2H), 4.13 (s, 1H), 4.38-4.41 (m, 1H), 5.38-5.43 (dd, *J* = 15.3, 5.8 Hz, 1H), 5.51-5.58 (m, 1H), 6.70-6.73 (t, *J* = 5.2 Hz, 1H), 7.18-7.21 (t, *J* = 7.3 Hz, 3H), 7.25-7.29 (t, *J* = 8.0 Hz, 5H), 7.38-7.40 (d, *J* = 7.6 Hz, 7H). **^{13}C NMR** (150 MHz, $CDCl_3$): δ 31.6, 31.7, 39.3, 42.6, 52.2, 66.8, 68.6,

69.4, 69.9, 70.3, 71.3, 126.8, 128.1, 129.8, 132.8, 145.1, 171.3, 172.3 ppm. **HRMS**: (ESI) calcd for $C_{33}H_{39}NO_6S$ $[M + Na]^+$ 600.2396; found 600.2389.

(*S,E*)-Methyl 6'-((3-hydroxy-7-(tritylthio)hept-4-enamido)methyl)-2,2'-bipyridine-6-carboxylate (68)

To a solution of the above obtained crude amine product **23** (729 mg, 3 mmol, 1 equiv) in dichloromethane (15 mL) was added DMAP (369 mg, 3 mmol, 1 equiv), and Hunig's base (390 mg, 3 mmol, 1 equiv). The reaction mixture was stirred at room temperature for 30 min before adding a solution of aldol product **30** (1.68 g, 3 mmol, 1 equiv) in dichloromethane (25 mL). The reaction mixture was stirred at room temperature overnight, concentrated in *vacuo*, and purified by flash chromatography on silica gel in ethyl acetate/hexanes (80-100%) to get **68** as a yellow oil (1.66 g, 85%). $[\alpha]_D^{22}$ + 1.7 (*c* 0.002, $CHCl_3$). **^{1}H NMR** (600 MHz, $CDCl_3$) δ 1.96 (brs, 1H), 2.07-2.10 (q, *J* = 8.4 Hz, 2H), 2.20-2.22 (t, *J* = 7.1 Hz, 2H), 2.46-2.55 (m, 2H), 3.77 (bb, 1H), 4.05 (s, 1H), 4.51 (m, 1H), 4.65-4.66 (d, *J* = 5.1 Hz, 2H), 5.46-5.49 (dd, *J* = 15.4, 6.2 Hz, 1H), 5.57-5.61 (dt, *J* = 15.2, 6.6 Hz, 1H), 7.20-7.23 (t, *J* = 7.3 Hz, 3H), 7.27-7.30 (t, *J* = 8.0 Hz, 6H), 7.40-7.42 (d, *J* = 7.6 Hz, 6H), 7.81-7.84 (t, *J* = 7.7 Hz, 1H), 7.94-7.97 (t, *J* = 7.9 Hz, 1H), 8.14-8.16 (dd, *J* = 7.7, 0.9 Hz, 1H), 8.42-8.44 (d, *J* = 7.7 Hz, 1H), 8.56-8.58 (dd, *J* = 8.1, 1.1 Hz, 1H). **^{13}C NMR** (150 MHz, $CDCl_3$): δ 31.3, 31.5, 42.7, 44.4, 53.0, 66.6, 69.3, 76.9, 77.1, 77.3, 120.4, 122.5, 124.3, 125.2, 126.7, 126.7, 127.9, 127.9, 129.6, 130.1, 132.4, 138.0, 144.8, 147.6, 154.5, 155.7, 156.0, 165.8, 171.9 ppm. **HRMS**: (ESI) calcd for $C_{39}H_{37}N_3O_4S$ $[M + Na]^+$ 666.2398; found 666.2371.

(*S*,*E*)-methyl 2-(((6-((3-hydroxy-7-(tritylthio)hept-4-enamido)methyl)pyridin-2-yl)methyl)(methyl)amino)acetate (69)

To a solution of the crude amine product **24** (1.25 g, 5.6 mmol, 1 equiv) in dichloromethane (25 mL) was added DMAP (690 mg, 5.6 mmol, 1 equiv), and Hunig's base (728 mg, 5.6 mmol, 1 equiv). The reaction mixture was stirred at room temperature for 30 min before adding a solution of the aldol product **30** (3.1 g, 5.5 mmol, 1 equiv) in dichloromethane (40 mL). The reaction mixture was stirred at room temperature overnight, concentrated in *vacuo* and purified by flash chromatography on silica gel in dichloromethane/ethyl acetate (30-50%) to get **69** as a yellow oil (2.97 g, 85%). $[\alpha]_D^{22}$= – 6.5 (*c* 0.02, $CHCl_3$). **^{1}H NMR** (600 MHz, $CDCl_3$) 2.08-2.11 (m, 2H), 2.21-2.24 (t, *J* = 7.5 Hz, 2H), 2.44 (s, 3H), 2.40-2.45 (m, 2H), 3.37 (s, 2H), 3.71 (s, 3H), 3.84 (s, 2H), 4.46-4.51 (m, 2H), 4.62-4.65 (dd, *J* = 6.5, 5.3 Hz, 1H), 5.45-5.49 (dd, *J* = 15.2, 6.1 Hz, 1H), 5.58-5.63 (m, 1H), 7.12-7.14 (d, *J* = 7.7 Hz, 1H), 7.20-7.23 (t, *J* = 9.1 Hz, 3H), 7.28-7.30 (t, *J* = 7.9 Hz, 6H), 7.33-7.34 (d, *J* = 7.7 Hz, 1H), 7.41-7.42 (d, *J* = 8.1 Hz, 6H), 7.63-7.66 (t, *J* = 7.5 Hz, 1H). **^{13}C NMR** (150 MHz, $CDCl_3$): δ 31.4, 31.5, 42.6, 43.0, 44.2, 51.6, 57.8, 62.3, 66.6, 69.1, 120.4, 121.9, 126.6, 127.9, 129.6, 132.7, 137.3, 144.9, 155.7, 157.9, 171.4, 172.1 ppm. **HRMS**: (ESI) calcd for $C_{37}H_{41}N_3O_4S$ $[M + H]^+$ 624.2896; found 624.2897.

(3*R*,16*S*)-3-Isopropyl-16-((*E*)-4-(tritylthio)but-1-enyl)-1,7,10-trioxa-4,13-diazacyclohexadecane-2,5,14-trione (75)

To a solution of **14** (35 mg, 0.040 mmol, 1 equiv) in THF/H_2O (4:1, 2 mL) at 0 ^oC was added 0.1M LiOH (0.4 mL, 0.04 mmol, 1.0 equiv) dropwise over a period of 10 minutes. The reaction mixture was stirred at 0 ^oC for another 1 h, treated with 1M HCl solution and extracted with

ethyl acetate (3 x 2 mL). The organic extract was washed with brine, dried over anhydrous sodium sulfate and solvent evaporated under reduced pressure to give the crude carboxylic acid, which was used in the next step without further purification.

To a solution of crude carboxylic acid in dichloromethane (5 mL) was added diethylamine (0.3 g, 3.9 mmol, 96 equiv). After stirring the reaction mixture at room temperature for 4 h, it was concentrated under reduced pressure and dried for 12 h in high vacuum to give the crude amine product. The crude product was used in the next step without additional purification.

A solution of the crude amine above, HATU (0.030 g, 0.08 mmol, 2.0 equiv), HOAt (11 mg, 0.08 mmol, 2.0 equiv), and Hunig's base (0.025 g, 0.187 mmol, 4.4 equiv) in dichloromethane (45 mL) was stirred for 3 days at room temperature. The reaction mixture was concentrated in *vacuo*, diluted with dichloromethane (5 mL), washed with brine, and solvent evaporated under reduced pressure. The residue was purified by flash chromatography on silica gel in ethyl acetate followed by recrystallization from dichloromethane/hexanes to give **75** as a white solid (17 mg, 65%). mp 183-188 ^{o}C. $[\alpha]_D^{20}$ – 2.34 (*c* 0.12, $CHCl_3$). **^{1}H NMR** (600 MHz, $CDCl_3$) δ 0.89-0.91 (d, *J* = 6.9 Hz, 3H), 0.95-0.96 (d, *J* = 6.9 Hz, 3H), 2.04-2.11 (m, 2H), 2.20-2.23 (t, *J* = 4.6 Hz, 2H), 2.32-2.37 (m, 1H), 2.48-2.52 (dd, *J* = 14.6, 9.1 Hz, 1H), 2.56-2.59 (dd, *J* = 14.6, 9.0 Hz, 1H), 3.31-3.35 (m, 1H), 3.48-3.56 (m, 2H), 3.61-3.70 (m, 3H), 3.72-3.76 (m, 2H), 3.96-3.98 (d, *J* = 15.7 Hz, 1H), 4.16-4.18 (d, *J* = 16.3 Hz, 1H), 4.80-4.83 (dd, *J* = 10.1, 4.3 Hz, 1H), 5.33-5.37 (m, 1H), 5.52-5.55 (m, 1H), 5.62-5.67 (m, 1H), 6.08-6.09 (m, 1H), 7.22-7.25 (tt, *J* = 16.6, 1.1 Hz, 3H), 7.29-7.34 (m, 6H), 7.41-7.43 (m, 6H). **^{13}C NMR** (150 MHz, $CDCl_3$): δ 17.2, 19.2, 19.2, 31.1, 31.4, 31.9, 38.9, 41.9, 56.6, 66.7, 68.8, 69.2, 70.0, 71.3, 71.6, 126.7, 127.7, 127.9, 129.6, 133.1, 144.8, 169.3, 169.3, 169.7 ppm. **HRMS**: (ESI) calcd for $C_{37}H_{44}N_2O_6S$ $[M + Na]^+$ 667.2818; found 667.2802.

(5*S*,8*S*)-5-isopropyl-8-((*E*)-4-(tritylthio)but-1-en-1-yl)-7-oxa-4,11-diaza-1,2(2,6)-dipyridinacyclododecaphane-3,6,10-trione (76)

To a solution of **15** (126 mg, 0.131 mmol, 1 equiv) in THF/H_2O (4:1, 2 mL) at 0 ^oC was added 0.1M LiOH (1.3 mL, 0.13 mmol, 1.0 equiv) dropwise over a period of 10 minutes. The reaction mixture was stirred at 0 ^oC for another 1 h, and 1M HCl solution (1.3 mL, 0.13 mmol, 1.0 equiv) was added. It was extracted with ethyl acetate and the organic extract was washed with brine, dried over anhydrous sodium sulfate and the solvent removed under reduced pressure to give the crude carboxylic acid which was used in the next step without further purification.

To a solution of the crude carboxylic acid in dichloromethane (5 mL) was added diethylamine (0.94 g, 12.5 mmol, 96 equiv). After stirring at room temperature for 12 h, the reaction mixture was concentrated under reduced pressure, and the residue was dried for 12 h in high *vacuo* to give the crude product, which was used in the next step without additional purification.

A mixture of the crude product obtained above, HATU (0.10 g, 0.26 mmol, 2.0 equiv), HOAt (0.036 g, 0.26 mmol, 2.0 equiv), and Hunig's base (0.075 g, 0.572 mmol, 4.4 equiv) in dichloromethane (130 mL) was stirred for 3 days at room temperature. It was concentrated in *vacuo* and diluted with dichloromethane (15 mL), washed with brine and evaporated under reduced pressure. The residue was partially purified by flash chromatography on silica gel in ethyl acetate to give **76** as a yellow oil (41 mg, 45%). **^{1}H NMR** (600 MHz, $CDCl_3$) δ 1.00-1.02 (d, *J* = 6.8 Hz, 3H), 1.04-1.05 (d, *J* = 6.8 Hz, 3H), 1.43-1.51 (m, 6H), 1.69-1.74 (m, 2H), 1.83 (bb, 1H), 1.87-1.96 (m, 2H), 2.39-2.42 (m, 1H), 3.18-3.2 (q, *J* = 7.3 Hz, 1H), 3.71-3.76 (m, 1H), 4.50-4.54 (dd, *J* = 17.2, 2.5 Hz, 1H), 4.84-4.89 (m, 2H), 5.33-5.37 (dd, *J* = 15.4, 5.3 Hz, 1H),

5.54-5.59 (dt, *J* = 15.6, 5.6 Hz, 1H), 5.76 (m, 1H), 7.17-7.20 (tt, *J* = 6.9, 1.5 Hz, 3H), 7.21-7.224 (dt, *J* = 7.0, 1.7 Hz, 6H), 7.25-7.27 (m, 5H), 7.29 (s, 1H), 7.39-7.41 (m, 1H), 7.83 (m, 2H), 7.00-8.02 (m, 2H), 8.18 (m, 1H), 9.66-9.68 (d, *J* = 9.9 Hz, 1H).

(7*S*,10*S*)-7-isopropyl-3-methyl-10-((*E*)-4-(tritylthio)but-1-en-1-yl)-9-oxa-3,6,13-triaza-1(2,6)-pyridinacyclotetradecaphane-5,8,12-trione (77)

To a solution of **16** (100 mg, 0.104 mmol, 1 equiv) in THF/H_2O (4:1, 2 mL) at 0 ^oC was added 0.1M LiOH (1.0 mL, 0.10 mmol, 1.0 equiv) drop wise over a period of 10 minutes. The reaction mixture was stirred at 0 ^oC for 1 h, after which a solution of 0.1M HCl (1.1 mL, 0.11 mmol, 1.1 equiv) was added and the reaction mixture was extracted with ethyl acetate. The organic extract was washed with brine, dried over anhydrous sodium sulfate and the solvent was removed under reduced pressure to give the crude carboxylic acid, which was used in the next step without further purification.

To a solution of the crude carboxylic acid in dichloromethane (5mL) was added diethylamine (0.72 g, 9.6 mmol, 96 equiv). After stirring at room temperature for 8 h, the reaction mixture was concentrated reduced pressure and dried in high vacuum to give the crude product. It was used in the next step without further purification.

To a mixture of the crude product obtained above, HATU (0.076 g, 0.20 mmol, 2.0 equiv), and HOAt (0.027 g, 0.20 mmol, 2.0 equiv) in dichloromethane (100 mL) was added Hunig's base (0.057 g, 0.44 mmol, 4.4 equiv). The reaction mixture was stirred for 3 days at room temperature, concentrated in *vacuo*, and diluted with dichloromethane. The dichloromethane solution was washed with brine and evaporated under reduced pressure. The residue was purified

by flash chromatography on silica gel in ethyl acetate to give **77** as a yellow oil (24 mg, 35%). $[\alpha]_D^{22}$ = - 18.2 (*c* 0.02, $CHCl_3$). **^{1}H NMR** (600 MHz, $CDCl_3$) δ 0.77-0.78 (d, *J* = 6.7 Hz, 3H), 0.88-0.99 (d, *J* = 6.8 Hz, 3H), 1.99-2.02 (q, *J* = 7.0 Hz, 2H), 2.11-2.16 (m, 2H), 2.22-2.37 (m, 2H), 2.30 (s, 3H), 2.62-2.66 (dd, *J* = 15.2 , 7.3 Hz, 1H), 2.75-2.77 (d, *J* = 13.6 Hz, 1H), 3.24-3.34 (q, *J* = 16.9 Hz, 2H), 3.54-3.56 (d, *J* = 13.4 Hz, 1H), 3.80-3.83 (d, *J* = 13.6 Hz, 1H), 4.56-4.59 (m, 2H), 4.82-4.84 (dd, *J* = 9.9, 4.2 Hz, 1H), 5.37-5.40 (dd, *J* = 15.3 , 6.1 Hz, 1H), 5.60 (m, 1H), 5.65-5.70 (dt, *J* = 15.4, 6.4 Hz, 1H), 7.10-7.13 (dd, *J* = 12.3, 7.0 Hz, 2H), 7.20-7.23 (t, *J* = 13.4 Hz, 3H), 7.28-7.29 (t, *J* = 2.9 Hz, 5H), 7.30-7.34 (m, 1H), 7.37-7.38 (d, *J* = 7.5 Hz, 5H), 7.40 (m, 1H), 7.43-7.47 (m, 1H), 7.64-7.66 (t, *J* = 7.5 Hz, 1H) 8.66-8.68 (d, *J* = 9.9 Hz, 1H). **^{13}C NMR** (150 MHz, $CDCl_3$): δ 17.5, 19.1, 31.1, 31.5, 32.5, 41.7, 42.8, 44.3, 57.0, 61.1, 62.9, 66.6, 71.9, 121.1, 122.0, 126.6, 127.4, 127.9, 129.6, 132.6, 137.3, 144.8, 155.6, 157.3, 169.1, 169.3, 170.4 ppm. **HRMS**: (ESI) calcd for $C_{41}H_{46}N_4O_4S$ $[M + Na]^+$ 713.3137; found 713.3167.

Single concentration HDAC isoform selectivity and dose-dependence screening

Primary HDAC1 antibody (Sigma Aldrich, H3284, final concentration 10µg/mL), primary HDAC2 antibody (Sigma Aldrich, H3159, final concentration 10µg/mL), primary HDAC3 antibody (Sigma Aldrich, H3034, final concentration 25µg/mL), or primary HDAC6 antibody (Sigma Aldrich, SAB1404771, final concentration 2µg/mL) were individually incubated in binding buffer (100µL final volume; 0.2M carbonate/0.2M bicarbonate buffer, pH 9.4) in wells of a high-capacity 96-well polystyrene white opaque plate (Thermo Scientific) either for 1 h at room temperature with gentle rocking (3 rpm), or overnight at 4 °C without rocking. For all reactions, unbound antibody was removed by washing quickly three times with 1X TBST buffer (400 µL, 50 mM Tris-HCl, 150 mM NaCl, pH 7.4, 0.05% (v/v) Tween-20), followed by a fourth

wash under the same conditions but with 5 minutes incubation and gentle rocking (3 rpm) at room temperature. The unbound regions of the wells were blocked with 5% non-fat dry milk in 1X TBST buffer (350 µL) for 1 h at room temperature with gentle rocking (3 rpm). To affix HDAC enzyme to the plate, HeLa cell lysates (100µL of 100µg/mL for HDAC1 and HDAC2, or 100µL of 1 mg/mL for HDAC3 and HDAC6 in 1X TBST buffer containing 0.1 % (w/v) non-fat dry milk) were added to each well and incubated for 1 h at 4 °C without rocking, followed by washing with 1X TBST (400 µL), as described previously. HDAC-Glo™ buffer (24 µL) was then added to the plate, with subsequent addition of the inhibitor in DMSO (1 µL), before incubation for 15 min at room temperature without rocking. An uninhibited control reaction was also included that contained DMSO alone (1 µL) in HDAC-Glo™ buffer (24 µL). Finally, deacetylase activity was measured using the HDAC-Glo™ assay kit (Promega) as per the manufacturer's protocol. The HDAC-Glo™ substrate (1 mL) and developer (1 µL) were first premixed and stored at -20°C. Then, to monitor deacetylase activity the pre-mixed HDAC-Glo™ reagents (25µL) was added to each well (50 µL total volume) and incubated for 30-45 min at room temperature without rocking. The concentrations of inhibitors reported in the single dose screen (Figure 6 and Table S14) and dose-dependent studies (Tables S16 and S18) are final concentrations after addition of HDAC-Glo™ reagent. The deacetylase activity was measured as luminescent signal using a GeniosPlus Fluorimeter (Tecan) at optimal gain. For each reaction, the luminescent signal was background corrected with the signal from a negative control reaction containing lysates, HDAC Glo™ buffer, and HDAC-Glo™ reagent, but no HDAC antibody in the initial antibody binding step. After background correction, percent deacetylase activity remaining was calculated by dividing the signal with inhibitor by the signal without inhibitor (DMSO negative control reaction), and then multiplying by 100. The mean percent deacetylase

activity along with standard error of at least two independent trials is reported in all figures and tables. IC_{50} values were calculated by fitting the percent deacetylase activity remaining as a function of inhibitor concentration to a sigmoidal dose-response curve ($y = 100/(1+(x/IC_{50})^Z)$, where y = percent deacetylase activity and x = inhibitor concentration) using non-linear regression with KaleidaGraph 4.1.3 software (Figure S15 and S17).

Computational Methods

Computational Methods

We previously reported results from a molecular dynamics (MD) simulation for HDAC-8 with a bound largazole analogue at its active site.[28] The study was based on the X-ray crystal structure (pdb ID:3RQD) in which a largazole molecule bound to HDAC-8 was in contact with another largazole bound to a second HDAC-8 found in the unit cell.[6] In the present study, the main players are HDAC-1, HDAC-2, and HDAC-6, it was our intention to study the ligand binding in these receptor proteins. However, only HDAC-1 {pdb ID: 4BKX} and HDAC-2 {pdb ID: 4LY1} have complete ligand binding domains available as X-ray crystal structures. Using our previously calculated solution structure of largazole thiol bound HDAC-8, largazole thiol was introduced to HDAC-1 and HDAC-2 ligand binding sites. Also, we made necessary in silico chemical structure modifications to largazole to obtain the initial structures of analogue **7**-thiol bound HDAC-1 and HDAC-2 structures. We performed a 50 ns molecular dynamics simulation for the largazole and analogue **7**-thiol bound to HDAC-1 and HDAC-2, based on these initial complexes.

The initial structure of isolated **7** was energy minimized at the B3LYP level with the cc-pvtz basis set using Gaussian-09[47] and the initial charges of the analogue for MD were derived from

this calculation. As mentioned above, this structure was used to guide replacing largazole thiol in the largazole thiol/HDAC-1 and largazole/HDAC-2 complexes. Each solvated complex containing the largazole thiol and analogue **7**-thiol with a thiol-coordinating Zn^{2+} ion bound to HDACs in each case and necessary Na+ ions (used to neutralize the central box that contained over 28000 water molecules) was subjected to an initial optimization/equilibration, followed by a 50 ns MD trajectory calculation using the PMEMD module of the program, Amber-14.[48] The FF14SB force field was used for the peptide atoms. Following our standard protocol, with particle mesh Ewald summation[49] for long range interactions and 1 fs time step, 5 ns NVT equilibration and 50 ns NPT production runs were carried out at 300K and 1atm. We also carried out two simulations with largazole alone in water and the analogue alone in water to estimate the binding enthalpies due to HDAC interaction. Configurations from the last 40 ns of dynamics were used for analysis.

Supporting Information

Molecular formula strings and associated biochemical and biological data, procedures for the synthesis of analogues **9**-**13**, Biological activity data, antiproliferative data for analogues **6**–**13**, Western blot analysis of global histome 3 acetylation, isoform selectivity data , ^{1}H NMR and ^{13}C NMR spectra for all compounds.

Corresponding Author

*Phone: +1 419 530-1983. E-mil: ltillek@utnet.utoledo.edu

Notes

The authors declare no competing financial interest.

ACKNOWLEDGEMENT:

This research was supported, in part, by the Intramural Research Program of the National Institute of Health, National Institute of Environmental Health Sciences grant Z01-ES043010 (to L.P) and NIH grant CA051085 (to RAC).

Abbreviatons Used:

HAT, histone acyl transferases; DIBAL-H, n-Bu-Li, n-butyllithium; $Pd(PPh_3)_4$, tetrakis(triphenylphosphine)palladium(0); Tosyl, *p*-toluenesulfonyl; HOAt, 1-hydroxy-7-azabenzotriazole; HATU, 1-[Bis(dimethylamino)methylene]-1H-1,2,3-triazolo[4,5-b]pyridinium 3-oxide hexafluorophosphate; MTS, 3-(4,5-dimethylthiazol-2-yl)-5-(3-carboxymethoxyphenyl)-2-(4-sulfophenyl)-2*H*-tetrazolium; EtOAc, ethyl acetate; LiOH, lithium hydroxide; NaN_3, sodium azide; TMSE, trimethylsiylethyl.

References:

(1) Jaenisch, R.; Bird, A. Epigenetic Regulation of Gene Expression: How the Genome Integrates Intrinsic and Environmental Signals. *Nat. Genet.* **2003**, *33 Suppl*, 245–254.

(2) Baylin, S. B.; Jones, P. A. A Decade of Exploring the Cancer Epigenome - Biological and Translational Implications. *Nat. Rev. Cancer* **2011**, *11* (10), 726–734.

(3) Egger, G.; Liang, G.; Aparicio, A.; Jones, P. A. Epigenetics in Human Disease and Prospects for Epigenetic Therapy. *Nature* **2004**, *429* (6990), 457–463.

(4) Strahl, B. D.; Allis, C. D. The Language of Covalent Histone Modifications. *Nature* **2000**, *403* (6765), 41–45.

(5) Conley, B. A.; Wright, J. J.; Kummar, S. Targeting Epigenetic Abnormalities with Histone Deacetylase Inhibitors. *Cancer* **2006**, *107* (4), 832–840.

(6) Cole, K. E.; Dowling, D. P.; Boone, M. A.; Phillips, A. J.; Christianson, D. W. Structural Basis of the Antiproliferative Activity of Largazole, a Depsipeptide Inhibitor of the Histone Deacetylases. *J. Am. Chem. Soc.* **2011**, *133* (32), 12474–12477.

(7) Falkenberg, K. J.; Johnstone, R. W. Histone Deacetylases and Their Inhibitors in Cancer, Neurological Diseases and Immune Disorders. *Nat. Rev. Drug Discov.* **2014**, *13* (9), 673–691.

(8) Zhang, J.; Zhong, Q. Histone Deacetylase Inhibitors and Cell Death. *Cell. Mol. Life Sci.* **2014**, *71* (20), 3885–3901.

(9) Choo, Q. Y.; Ho, P. C.; Lin, H. S. Histone Deacetylase Inhibitors: New Hope for Rheumatoid Arthritis? *Curr. Pharm. Des.* **2008**, *14* (8), 803–820.

(10) Wiech, N. L.; Fisher, J. F.; Helquist, P.; Wiest, O. Inhibition of Histone Deacetylases: A Pharmacological Approach to the Treatment of Non-Cancer Disorders. *Curr. Top. Med. Chem.* **2009**, *9* (3), 257–271.

(11) Marks, P. A. Discovery and Development of SAHA as an Anticancer Agent. *Oncogene* **2007**, *26*, 1351–1356.

(12) Bertino, E. M.; Otterson, G. A. Romidepsin: A Novel Histone Deacetylase Inhibitor for Cancer. *Expert Opin. Investig. Drugs* **2011**, *20*, 1151–1158.

(13) Goldenberg, M. M. Pharmaceutical Approval Update. *P T* **2014**, *39* (9), 619–620,626.

(14) Torimoto, Y.; Shindo, M.; Ikuta, K.; Kohgo, Y. Current Therapeutic Strategies for Multiple Myeloma. *Int. J. Clin. Oncol.* **2015**. 20 (3), 423-430.

(15) Thiagalingam, S.; Cheng, K. H.; Lee, H. J.; Mineva, N.; Thiagalingam, A.; Ponte, J. F. Histone Deacetylases: Unique Players in Shaping the Epigenetic Histone Code. *Ann. N. Y. Acad. Sci.* **2003**, *983*, 84–100.

(16) Bieliauskas, A. V; Pflum, M. K. Isoform-Selective Histone Deacetylase Inhibitors. *Chem. Soc. Rev.* **2008**, *37* (7), 1402–1413.

(17) Miller, T. A.; Witter, D. J.; Belvedere, S. Histone Deacetylase Inhibitors. *J. Med. Chem.* **2003**, *46* (24), 5097–5116.

(18) Taori, K.; Paul, V. J.; Luesch, H. Structure and Activity of Largazole, a Potent Antiproliferative Agent from the Floridian Marine Cyanobacterium Symploca Sp. *J. Am. Chem. Soc.* **2008**, *130* (6), 1806–1807.

(19) Ahmed, S.; Riegsecker, S.; Beamer, M.; Rahman, A.; Bellini, J. V.; Bhansali, P.; Tillekeratne, L. M. V. Largazole, a Class I Histone Deacetylase Inhibitor, Enhances TNF-??-Induced ICAM-1 and VCAM-1 Expression in Rheumatoid Arthritis Synovial Fibroblasts. *Toxicol. Appl. Pharmacol.* **2013**, *270*, 87–96.

(20) Zhou, H.; Jiang, S.; Chen, J.; Ren, X.; Jin, J.; Su, S. B. Largazole, an Inhibitor of Class I Histone Deacetylases, Attenuates Inflammatory Corneal Neovascularization. *Eur. J. Pharmacol.* **2014**, *740*, 619–626.

(21) Liu, Y.; Wang, Z.; Wang, J.; Lam, W.; Kwong, S.; Li, F.; Friedman, S. L.; Zhou, S.; Ren, Q.; Xu, Z.; Wang, X.; Ji, L.; Tang, S.; Zhang, H.; Lui, E. L.; Ye, T. A Histone Deacetylase Inhibitor, Largazole, Decreases Liver Fibrosis and Angiogenesis by Inhibiting Transforming Growth Factor-Beta and Vascular Endothelial Growth Factor Signalling. *Liver. Int.* **2013**, *33* (4), 504–515.

(22) Li, S.; Yao, H. Q.; Xu, J. Y.; Jiang, S. Synthetic Routes and Biological Evaluation of Largazole and Its Analogues as Potent Histone Deacetylase Inhibitors. *Molecules* **2011**, *16* (6), 4681–4694.

(23) Hong, J. Y.; Luesch, H. Largazole: From Discovery to Broad-Spectrum Therapy. *Nat. Prod. Rep.* **2012**, *29* (4), 449–456.

(24) Chen, F.; Chai, H.; Su, M. B.; Zhang, Y. M.; Li, J.; Xie, X.; Nan, F. J. Potent and Orally Efficacious Bisthiazole-Based Histone Deacetylase Inhibitors. *ACS Med. Chem. Lett.* **2014**, *5*, 628–633.

(25) Salvador, L. A.; Park, H.; Al-Awadhi, F. H.; Liu, Y.; Kim, B.; Zeller, S. L.; Chen, Q. Y.; Hong, J.; Luesch, H. Modulation of Activity Profiles for Largazole-Based HDAC Inhibitors through Alteration of Prodrug Properties. *ACS Med. Chem. Lett.* **2014**, *5* (8), 905–910.

(26) Kim, B.; Park, H.; Salvador, L. A.; Serrano, P. E.; Kwan, J. C.; Zeller, S. L.; Chen, Q.-Y.; Ryu, S.; Liu, Y.; Byeon, S.; Luesch, H.; Hong, J. Evaluation of Class I HDAC Isoform Selectivity of Largazole Analogues. *Bioorg. Med. Chem. Lett.* **2014**, *24* (16), 3728–3731.

(27) Bhansali, P.; Hanigan, C. L.; Casero, R. A.; Tillekeratne, L. M. V. Largazole and Analogues with Modified Metal-Binding Motifs Targeting Histone Deacetylases: Synthesis and Biological Evaluation. *J. Med. Chem.* **2011**, *54*, 7453–7463.

(28) Bhansali, P.; Hanigan, C. L.; Perera, L.; Casero, R. A.; Tillekeratne, L. M. V. Synthesis and Biological Evaluation of Largazole Analogues with Modified Surface Recognition Cap Groups. *Eur. J. Med. Chem.* **2014**, *86*, 528–541.

(29) Reddy Damodara, N.; Ballante, F.; Chuang, T.; Marshall Garland, R.; Pirolli, A.;

Marrocco, B. Design and Synthesis of Simplified Largazole Analogues as Isoform-Selective Human Lysine Deacetylase Inhibitors. *J. Med. Chem.* **2016**, *59* (4), 1613–1633.

(30) Zeng, X.; Yin, B.; Hu, Z.; Liao, C.; Liu, J.; Li, S.; Li, Z.; Nicklaus, M. C.; Zhou, G.; Jiang, S. Total Synthesis and Biological Evaluation of Largazole and Derivatives with Promising Selectivity for Cancers Cells. *Org. Lett.* **2010**, *12* (6), 1368–1371.

(31) Ying, Y.; Liu, Y.; Byeon, S. R.; Kim, H.; Luesch, H.; Hong, J. Synthesis and Activity of Largazole Analogues with Linker and Macrocycle Modification. *Org. Lett.* **2008**, *10* (18), 4021–4024.

(32) Bowers, A. A.; West, N.; Newkirk, T. L.; Troutman-Youngman, A. E.; Schreiber, S. L.; Wiest, O.; Bradner, J. E.; Williams, R. M. Synthesis and Histone Deacetylase Inhibitory Activity of Largazole Analogs: Alteration of the Zinc-Binding Domain and Macrocyclic Scaffold. *Org. Lett.* **2009**, *11* (6), 1301–1304.

(33) Benelkebir, H.; Marie, S.; Hayden, A. L.; Lyle, J.; Loadman, P. M.; Crabb, S. J.; Packham, G.; Ganesan, A. Total Synthesis of Largazole and Analogues: HDAC Inhibition, Antiproliferative Activity and Metabolic Stability. *Bioorg. Med. Chem.* **2011**, *19* (12), 3650–3658.

(34) Wang, B.; Huang, P.-H.; Chen, C.-S.; Forsyth, C. J. Total Syntheses of the Histone Deacetylase Inhibitors Largazole and 2-Epi-Largazole: Application of N-Heterocyclic Carbene Mediated Acylations in Complex Molecule Synthesis. *J. Org. Chem.* **2011**, *76* (4), 1140–1150.

(35) Souto, J. A.; Vaz, E.; Lepore, I.; Poppler, A. C.; Franci, G.; Alvarez, R.; Altucci, L.; de Lera, A. R. Synthesis and Biological Characterization of the Histone Deacetylase Inhibitor

Largazole and C7- Modified Analogues. *J. Med. Chem.* **2010**, *53* (12), 4654–4667.

(36) Bowers, A.; West, N.; Taunton, J.; Schreiber, S. L.; Bradner, J. E.; Williams, R. M. Total Synthesis and Biological Mode of Action of Largazole: A Potent Class I Histone Deacetylase Inhibitor. *J. Am. Chem. Soc.* **2008**, *130* (33), 11219–11222.

(37) Ying, Y.; Taori, K.; Kim, H.; Hong, J.; Luesch, H. Total Synthesis and Molecular Target of Largazole, a Histone Deacetylase Inhibitor. *J. Am. Chem. Soc.* **2008**, *130* (26), 8455–8459.

(38) Cha, J. S.; Kwon, O. O.; Jeoung, M. K.; Kim, E. J. Conversion of Nitriles into Aldehydes by Diisobutylaluminum Hydride-Dimethyl Sulfide Complex. *Bull. Korean Chem. Soc.* **1994**, *15* (11), 1021–1023.

(39) Hoye, T. R.; Jeffrey, C. S.; Shao, F. Mosher Ester Analysis for the Determination of Absolute Configuration of Stereogenic (Chiral) Carbinol Carbons. *Nat. Protoc.* **2007**, *2*, 2451–2458.

(40) Baughman, T. W.; Sworen, J. C.; Wagener, K. B. The Facile Preparation of Alkenyl Metathesis Synthons. *Tetrahedron* **2004**, *60*, 10943–10948.

(41) Andreiadis, E. S.; Demadrille, R.; Imbert, D.; Pecaut, J.; Mazzanti, M. Remarkable Tuning of the Coordination and Photophysical Properties of Lanthanide Ions in a Series of Tetrazole-Based Complexes. *Chemistry (Easton).* **2009**, *15* (37), 9458–9476.

(42) Zhang, T. Z.; Anslyn, E. V. Molecular Recognition and Indicator-Displacement Assays for Phosphoesters. *Tetrahedron* **2004**, *60* (49), 11117–11124.

(43) Sharma, S. K.; Wu, Y.; Steinbergs, N.; Crowley, M. L.; Hanson, A. S.; Casero, R. A.; Woster, P. M. (Bis)urea and (Bis)thiourea Inhibitors of Lysine-Specific Demethylase 1 as

Epigenetic Modulators. *J. Med. Chem.* **2010**, *53* (14), 5197–5212.

(44) Shoemaker, R. H. The NCI60 Human Tumour Cell Line Anticancer Drug Screen. *Nat. Rev. Cancer* **2006**, *6*, 813–823.

(45) Liu, Y.; Salvador, L. A.; Byeon, S.; Ying, Y.; Kwan, J. C.; Law, B. K.; Hong, J.; Luesch, H. Anticolon Cancer Activity of Largazole, a Marine-Derived Tunable Histone Deacetylase Inhibitor. *J. Pharmacol. Exp. Ther.* **2010**, *335* (2), 351–361.

(46) Padige, G.; Negmeldin, A. T.; Pflum, M. K. Development of an ELISA-Based HDAC Activity Assay for Characterization of Isoform-Selective Inhibitors. *J. Biomol. Screen.* **2015**, *20* (10), 1277–1285.

(47) Millard, C. J.; Watson, P. J.; Celardo, I.; Gordiyenko, Y.; Cowley, S. M.; Robinson, C. V; Fairall, L.; Schwabe, J. W. Class I HDACs Share a Common Mechanism of Regulation by Inositol Phosphates. *Mol. Cell* **2013**, *51* (1), 57–67.

(48) Lauffer, B. E.; Mintzer, R.; Fong, R.; Mukund, S.; Tam, C.; Zilberleyb, I.; Flicke, B.; Ritscher, A.; Fedorowicz, G.; Vallero, R.; Ortwine, D. F.; Gunzner, J.; Modrusan, Z.; Neumann, L.; Koth, C. M.; Lupardus, P. J.; Kaminker, J. S.; Heise, C. E.; Steiner, P. Histone Deacetylase (HDAC) Inhibitor Kinetic Rate Constants Correlate with Cellular Histone Acetylation but Not Transcription and Cell Viability. *J. Biol. Chem.* **2013**, *288* (37), 26926–26943.

(49) Marenich, A. V; Jerome, S. V; Cramer, C. J.; Truhlar, D. G. Charge Model 5: An Extension of Hirshfeld Population Analysis for the Accurate Description of Molecular Interactions in Gaseous and Condensed Phases. *J. Chem. Theory Comput.* **2012**, *8* (2), 527–541.

(50) Lane, A. A.; Chabner, B. A. Histone Deacetylase Inhibitors in Cancer Therapy. *J. Clin. Oncol.* **2009**, *27* (32), 5459–5468.

(51) Methot, J. L.; Chakravarty, P. K.; Chenard, M.; Close, J.; Cruz, J. C.; Dahlberg, W. K.; Fleming, J.; Hamblett, C. L.; Hamill, J. E.; Harrington, P.; Harsch, A.; Heidebrecht, R.; Hughes, B.; Jung, J.; Kenific, C. M.; Kral, A. M.; Meinke, P. T.; Middleton, R. E.; Ozerova, N.; Sloman, D. L.; Stanton, M. G.; Szewczak, A. A.; Tyagarajan, S.; Witter, D. J.; Secrist, J. P.; Miller, T. A. Exploration of the Internal Cavity of Histone Deacetylase (HDAC) with Selective HDAC1/HDAC2 Inhibitors (SHI-1 : 2). *Bioorg. Med. Chem. Lett.* **2008**, *18* (3), 973–978.

(52) Whitehead, L.; Dobler, M. R.; Radetich, B.; Zhu, Y.; Atadja, P. W.; Claiborne, T.; Grob, J. E.; McRiner, A.; Pancost, M. R.; Patnaik, A.; Shao, W.; Shultz, M.; Tichkule, R.; Tommasi, R. A.; Vash, B.; Wang, P.; Stams, T. Human HDAC Isoform Selectivity Achieved via Exploitation of the Acetate Release Channel with Structurally Unique Small Molecule Inhibitors. *Bioorg. Med. Chem.* **2011**, *19* (15), 4626–4634.

(53) Pilon, J. L.; Clausen, D. J.; Hansen, R. J.; Lunghofer, P. J.; Charles, B.; Rose, B. J.; Thamm, D. H.; Gustafson, D. L.; Bradner, J. E.; Williams, R. M. Comparative Pharmacokinetic Properties and Antitumor Activity of the Marine HDACi Largazole and Largazole Peptide Isostere. *Cancer Chemother. Pharmacol.* **2015**, *75* (4), 671–682.

Table of Contents Graphic

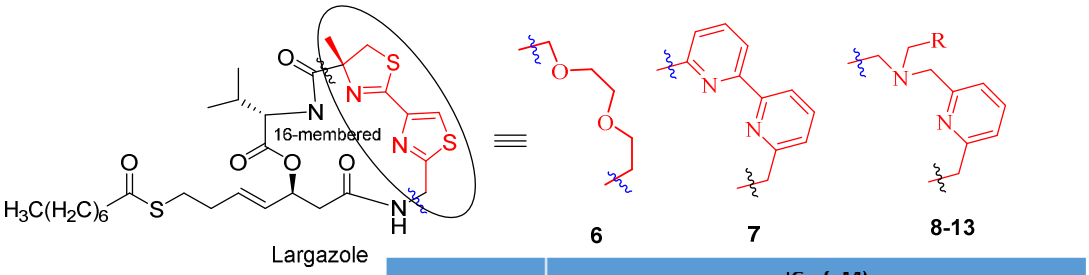

Compound	IC_{50} (nM)			
	HDAC1	HDAC2	HDAC3	HDAC6
Largazole	61	64	50	1400
7	**21**	28	27	13000